Available online at www.sciencedirect.com
ScienceDirect
Coordination Chemistry Reviews 252 (2008) 1121–1152
COORDINATION CHEMISTRY REVIEWS
www.elsevier.com/locate/ccr

Review

Polynuclear metal complexes of ligands containing phenolic units

Gianluca Ambrosi, Mauro Formica, Vieri Fusi *, Luca Giorgi, Mauro Micheloni *

Chemical Sciences Institute, University of Urbino, P.za Rinascimento 6, I-61029 Urbino, Italy

Received 26 June 2007; accepted 27 September 2007
Available online 2 October 2007

Contents

Abstract

The coordination properties of a selected series of acyclic and macrocyclic ligands containing one or more phenolic groups are explored. The formation of polynuclear metal complexes was only considered highlighting the key role played by the phenoxide oxygen atom in binding two metal centres in a bridge disposition. This arrangement allows two metal ions to stay close each other and consequently these dinuclear centres are able to mimic many biological sites, especially those where the two metals can cooperate to form an active centre. Catalytic properties of these polynuclear complexes, when studied, have been reported. Also some of the numerous heterodinuclear metal complexes that have been synthesized are here reviewed, included several crystal structures.

Keywords: Metal complexes; Phenol; Thermodynamics

Abbreviations: Ac, acetyl group; $acac^-$, acetylacetonate anion; binol, binaphtol; bpy, 2,2′-bipyridil; DACO, 1,5-diazacyclooctane; DMF, *N*,*N*-dimethylformamide; Et, ethyl group; Fc^+/Fc, ferrocenium/ferrocene red-ox couple; HBNP, bis(*p*-nitrophenyl)hydrogenphosphate; hfa^-, hexafluoroacetylacetonate anion; Hiso, isonicotinic acid; iNOS, inducible nitric oxide synthase; Iso^-, isonicotinate anion; LL, generic bidentate ligand; Ln, lanthanide metal; LPS, lipopolysaccharide; Me, methyl group; $mpdp^{2-}$, *m*-phenylene dipropionate anion; OEC, oxygen evolving centre; PAPs, purple acid phosphatase; Ph, phenyl group; Pr, propyl group; Py, pyridine; RAW 264.7, monocyte macrophage cell line; SCE, saturated calomel electrode; solv, generic coordinate solvent; *t*Bu, *t*-butyl group; TNP, tris(*p*-nitrophenyl)phosphate.

* Corresponding author. Tel.: +39 0722 350032; fax: +39 0722 350032.
E-mail address: mauro@uniurb.it (M. Micheloni).

0010-8545/$ – see front matter © 2007 Elsevier B.V. All rights reserved.
doi:10.1016/j.ccr.2007.09.027

1. Introduction

Polynucleating ligands are a growing class of compounds; this term, firstly coined as "dinucleating ligands" by Robson [1] in 1970, defines a class of ligands able to simultaneously bind two or more metal ions thus forming di- or polynuclear metal complexes. In this field, not only the ligands, but also their coordination compounds were extensively investigated allowing the understanding of the basic metal–metal interactions. The possible applications of the complexes formed by this type of ligands vary from the biomimetic studies of dinuclear metalloproteins or hosting and carrying of small molecules to their interesting catalytic properties.

Among many different types of dinucleating ligands, and more generally polynucleating ligands, the phenol-based molecules have attracted particularly a great number of researchers. This is due to the key role played by the phenolic group which has many useful electronic and structural characteristics such as: (i) charge as function of pH, spanning from 0 at low pH to −1 at high pH values; (ii) bridging capability, often the phenolic donor atom binds two metal centres in close proximity; (iii) the benzene ring present allows a great synthetic flexibility.

Regarding the first point, the acid–base properties of the phenol in aqueous solution depends on the ligand topology in which it is inserted; in fact, although the phenol loses its acidic proton at pH > 10 giving the phenolate $H_{-1}L^-$ anionic species (the reaction is $L = H_{-1}L^- + H^+$), this process can occur also at lower pH values when the phenol takes part of an amino-phenolic ligand. Often, it is the $H_{-1}L$ species involved in the second point, that is the phenolate oxygen atom to bridge two metal centres.

2. Acyclic ligands

2.1. Ligands containing one phenolic unit

2.1.1. Ligand forming μ-phenoxo dinuclear complexes

Dinuclear metal complexes have been the subject of extensive investigations due to their applications in many chemical fields. In fact, dinuclear metal complexes are successful devices for the recognition and assembly of external species of different nature such as inorganic and organic species. Many natural biological sites, such as the active centres of various metalloenzymes, are produced by the two transition metal ions; thus synthetic dinuclear receptors can be used to mimic the active centres. The important factors for the coordination and/or activation of secondary species are an unsaturated coordination environment of the two metals ions, and the preorganization of the receptor to host the new species. The distance between the two metal ions is crucial to allow the cooperation of both metal ions in forming the active centre. Due to bridging abilities of the phenolate oxygen atom towards metal ions, an important class of acyclic ligands capable to bind two metal ions close to each other, contains one phenol unit.

Table 1
Protonation constants (log *K*) of **L1** determined by means of potentiometric measurements in 0.15 mol dm^{-3} NMe_4Cl aqueous solution at 298.1 K

Reaction	log *K*
$\mathbf{L1} + H^+ = H\mathbf{L1}^+$	10.49(1)[a]
$H\mathbf{L1}^+ + H^+ = H_2\mathbf{L1}^{2+}$	9.68(1)
$H_2\mathbf{L1}^{2+} + H^+ = H_3\mathbf{L1}^{3+}$	9.21(1)
$H_3\mathbf{L1}^{3+} + H^+ = H_4\mathbf{L1}^{4+}$	7.59(1)
$H_4\mathbf{L1}^{4+} + H^+ = H_5\mathbf{L1}^{5+}$	2.31(3)

[a] Values in parentheses are the standard deviations on the last significant figure.

2.1.1.1 Phenolic ligands bearing polyamine side-arms.

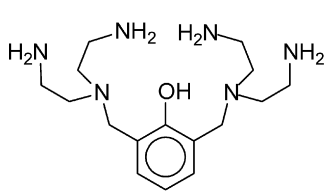

L1

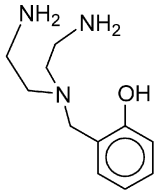

L2

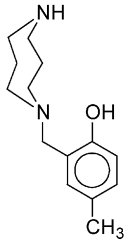

L3

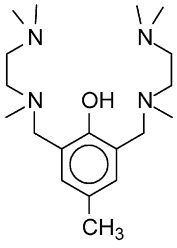

L4

The basicity behaviour and coordination properties in aqueous solution of the ligand **L1** (2,6-bis{[bis(2-aminoethyl)amino] methyl}phenol) towards Co(II), are reported and discussed together with those of the species formed with Ni(II), Cu(II) and Zn(II) ions (Tables 1 and 2).

The dinuclear Co(II) complexes of **L1** were studied as possible binders for molecular dioxygen (Table 3) [2]. The studies were carried out using potentiometric measurements (298.1 K, $I = 0.15$ mol dm^{-3}), UV–visible absorption spectra, and ^1H and ^{13}C NMR spectra in aqueous solution. **L1** behaves as a pentaprotic base in the range of the potentiometric measurements; the UV and NMR experiments revealed that in **L1**, $H\mathbf{L1}^+$, $H_2\mathbf{L1}^{2+}$, and $H_3\mathbf{L1}^{3+}$ species there is the simultaneous presence of positive and one negative charge on the ligand.

L1 forms mono and dinuclear complexes with Co(II) ion. The dinuclear species occur with the complete deprotonation of the ligand; the oxygen atom of the phenolate moiety bridges the two metal ions forcing them to stay close to each other, preorganizing the complexes to bind an additional molecule.

This is the case of the dinuclear Co(II) species $[Co_2(H_{-1}\mathbf{L1})(OH)j]^{(3-j)+}$ ($j = 0$–2), which cooperate to bind one molecule of dioxygen, giving rise to mono-oxygenated species. The stoichiometry of such species $[Co_2(H_{-1}\,\mathbf{L1})(OH)jO_2]^{(3-j)+}$ ($j = 0$–2), and other experimental data are in agreement with the formation of μ-peroxo complexes where the O_2 molecule

Table 2
Logarithm of the equilibrium constants determined in 0.15 mol dm^{-3} NMe_4Cl at 298.1 K for the complexation reactions of **L1** with Co(II), Ni(II), Cu(II) and Zn(II) ions

Reaction	log *K*			
	Co(II)	Ni(II)	Cu(II)	Zn(II)
$M^{2+} + \mathbf{L1} = M\mathbf{L1}^{2+}$	13.81(2)[a]	15.13(2)	21.01(1)	14.87(4)
$M\mathbf{L1}^{2+} + H^+ = M(H\mathbf{L1})^{3+}$	8.65(2)	8.83(2)	7.26(1)	8.64(3)
$M(H\mathbf{L1})^{3+} + H^+ = M(H_2\mathbf{L1})^{4+}$	5.06(7)	4.68(1)	4.75(1)	5.16(4)
$M(H_2\mathbf{L1})^{4+} + H^+ = M(H_3\mathbf{L1})^{5+}$			3.59(1)	
$M\mathbf{L1}^{2+} + H_2O = M(H_{-1}\mathbf{L1})^{+} + H_3O^+$	−9.57(1)	−9.64(1)	−9.41(1)	−9.24(1)
$M^{2+} + M\mathbf{L1}^{2+} = M_2\mathbf{L1}^{4+}$			9.26(1)	
$M^{2+} + M(H_{-1}\mathbf{L1})^{+} = M_2(H_{-1}\mathbf{L1})^{3+}$	10.01(1)	10.45(1)	14.35(1)	12.01(1)
$M_2(H_{-1}\mathbf{L1})^{3+} + OH^- = M_2(H_{-1}\mathbf{L1})OH^{2+}$	5.16(1)	5.18(1)	7.65(1)	5.17(1)
$M_2(H_{-1}\mathbf{L1})OH^{2+} + OH^- = M_2(H_{-1}\mathbf{L1})(OH)_2{}^+$	2.78(1)			

[a] Values in parentheses are the standard deviations on the last significant figure.

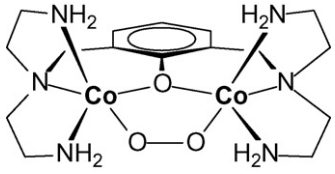

Fig. 1. Proposed coordination model of the $[Co_2(H_{-1}\mathbf{L1})(\mu\text{-}O_2)]^{3+}$ complex.

Table 3
Logarithm of the equilibrium constants determined in 0.15 mol dm^{-3} NMe_4Cl at 298.1 K for the complexation reactions of the oxygenated cobalt complexes

Reaction	log *K*
$2Co^{2+} + \mathbf{L1} + H_2O = Co_2(H_{-1}\mathbf{L1})(\mu\text{-}O_2)^{3+} + H_3O^+$	18.02(4)[a]
$2Co^{2+} + \mathbf{L1} + 3H_2O = Co_2(H_{-1}\mathbf{L1})(OH)(\mu\text{-}O_2)^{2+} + 2H_3O^+$	9.96(5)
$2Co^{2+} + \mathbf{L1} + 5H_2O = Co_2(H_{-1}\mathbf{L1})(OH)_2(\mu\text{-}O_2)^{+} + 3H_3O^+$	−0.45(7)
$Co_2(H_{-1}\mathbf{L1})^{3+} + O_2 = Co_2(H_{-1}\mathbf{L1})(\mu\text{-}O_2)^{3+}$	3.77
$Co_2(H_{-1}\mathbf{L1})OH^{2+} + O_2 = Co_2(H_{-1}\mathbf{L1})(OH)(\mu\text{-}O_2)^{2+}$	4.28
$Co_2(H_{-1}\mathbf{L1})(OH)_2{}^+ + O_2 = Co_2(H_{-1}\mathbf{L1})(OH)_2(\mu\text{-}O_2)^{+}$	4.82
$Co_2(H_{-1}\mathbf{L1})(\mu\text{-}O_2)^{3+} + OH^- = Co_2(H_{-1}\mathbf{L1})(OH)(\mu\text{-}O_2)^{2+}$	5.67
$Co_2(H_{-1}\mathbf{L1})(OH)(\mu\text{-}O_2)^{2+} + OH^- = Co_2(H_{-1}\mathbf{L1})(OH)_2(\mu\text{-}O_2)^{+}$	3.32

[a] Values in parentheses are the standard deviations on the last significant figure.

bridges the two metal ions (Fig. 1). The experiments showed that the oxygenation reactions are reversible.

The coordination properties of the ligand **L1** towards the Zn(II) ion were determined by potentiometric measurements in aqueous solution (Table 2, 298.1 K, $I = 0.15$ mol dm^{-3}).

L1 forms mono- and dinuclear complexes with Zn(II) ion [3,4]. The stable dinuclear complexes are practically the only existing species using **L1**/Zn(II), molar ratio of 1:2. In these species, each dien subunit binds one Zn(II) ion, while the phenolate moiety bound to both ions allows the two metal centres to be in close proximity with an incomplete coordination environment, the Zn(II)–Zn(II) separation is of 3.090 Å. The role of this metal–metal distance in binding secondary ligands was studied for the dinuclear systems 2Zn/**L1** and 2Cu/**L1** by potentiometric (Table 4, 298.1 K, $I = 0.15$ mol dm^{-3}) and NMR experiments in aqueous and MeOH solution with small guests having N donor atoms. The coordination sphere of the two metal ions was completed by adding one equiv of only those guests, which showed at least two contiguous donor atoms or two lone pairs on the same atom, to exactly match the metal–metal distance without modifying the metal cluster. To do this, the imidazole molecule which shows the highest addition constants to the $[M_2(H_{-1}\mathbf{L1})]^{3+}$ species probably forms a μ-1,1-amino. These results are in agreement with the two crystal structures reported herein $[Zn_2(H_{-1}\mathbf{L1})(CH_3CH_2CH_2CH_2O)](ClO_4)_2$ and $[Zn_2(H_{-1}\mathbf{L1})(N_3)](ClO_4)_2$. In fact, these structures display a butanolate or azide guest linked to both Zn(II) ions of the dinuclear complex, resulting in a μ-1,1-oxo and μ-1,1-azido bridge, respectively (Fig. 2).

The Ni(II) dinuclear complexes of **L1** $[Ni_2(H_{-1}\mathbf{L1})Cl_3]$ is a neutral species in which the two Ni(II) ions are bridged by the oxygen atom of the phenolato moiety and by a μ-chloride anion

Table 4
Logarithm of the formation constants for the 2Cu(II)/**L1** and 2Zn(II)/**L1** systems with the guests G, determined in 0.15 mol dm^{-3} NMe_4Cl at 298.1 K

Reaction	log *K*				
	Cu(II)			Zn(II)	
	Imidazole	Pyrazole	Pyridazine	Pyrazole	Azide
$2M^{2+} + \mathbf{L1} + G = M_2(H_{-1}\mathbf{L1})G^{3+} + H^+$	30.57(3)[a]	29.10(4)	28.54(2)	21.68(3)	20.45(2)
$2M^{2+} + \mathbf{L1} + G = M_2(H_{-1}\mathbf{L1})(H_{-1}G)^{3+} + H^+$	23.64(4)	24.24(4)	23.90(3)	13.06(3)	
$2M^{2+} + \mathbf{L1} + G = M_2(H_{-1}\mathbf{L1})(H_{-2}G)^{3+} + H^+$	12.51(3)	13.08(3)		2.97(4)	
$M_2(H_{-1}\mathbf{L1})^{3+} + G = M_2(H_{-1}\mathbf{L1})G^{3+}$	4.6	3.2	2.6	4.0	2.8

[a] Values in parentheses are the standard deviations on the last significant figure.

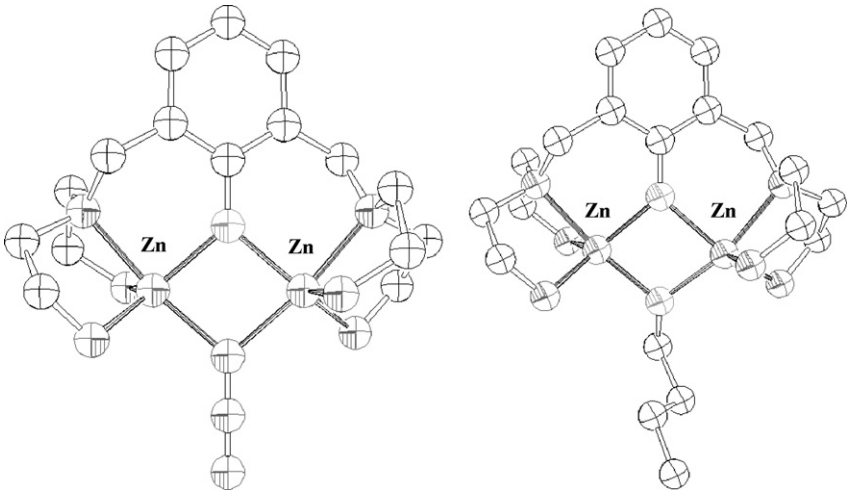

Fig. 2. ORTEP view of the complex cations $[Zn_2(H_{-1}\mathbf{L1})CH_3CH_2CH_2CH_2O)]^{2+}$ and $[Zn_2(H_{-1}\mathbf{L1})N_3]^{2+}$.

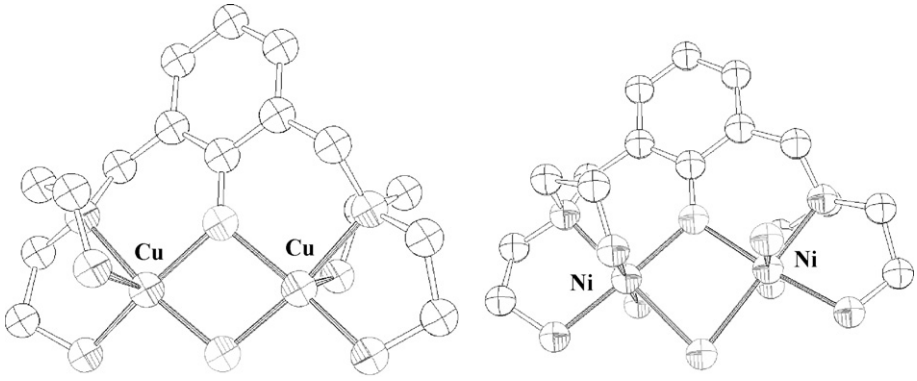

Fig. 3. ORTEP view of the complex cation $[Cu_2(H_{-1}\mathbf{L1})OH]^{2+}$ and $[Ni_2(H_{-1}\mathbf{L1})Cl_3]$ species.

[5]. The coordination around each Ni(II) ion is completed by binding a further chloride anion, the Ni(II)–Ni(II) distance is of 3.226 Å (Fig. 3).

In the Cu(II) dinuclear complexes of **L1** $[Cu_2(H_{-1}\mathbf{L1})OH](ClO_4)_2$ the two Cu(II) ions are bridged by the oxygen atom of the phenolato moiety and by one μ-OH^- ion, with a Cu(II)–Cu(II) separation of 3.004 Å (Fig. 3). This dinuclear copper complex has been also used as scavenger of nitric oxide in biological medium. Nitric oxide is a gaseous, short-living free radical which behaves as an important signalling molecule with pleiotropic capacities including vasodilatation, neurotransmission, and microbial and tumour cell killing, as well as in tissue damage and organ-specific autoimmune disorders. The stability constants of **L1** with Cu(II) ion were also determined by potentiometric measurements in aqueous solution (310.1 K, $I = 0.15$ M of NaCl) to mimic the biological medium (Tables 5 and 6). The measurements demonstrated that the $[Cu_2(H_{-1}\mathbf{L1})OH]^{2+}$ is the predominant species present in solution at pH 7.4.

The molecular structure of this species suggests the cooperation of the two copper ions in assembling the substrate, thus the complex can be used as a receptor for small molecules such as NO [6,7].

As a biological model, the authors chose the production of NO catalyzed by inducible nitric oxide synthase obtained from RAW 264.7 murine macrophage cell line stimulated with LPS. The experiments proved that NO is coordinated by the complex $[Cu_2(H_{-1}\mathbf{L1})OH]^{2+}$. The coor-

Table 5
Protonation constants (log K) of **L1** determined by means of potentiometric measurements in 0.15 mol dm^{-3} NaCl aqueous solution at 310.1 K

Reaction	log K
$\mathbf{L1} + H^+ = H\mathbf{L1}^+$	10.47(1)[a]
$H\mathbf{L1}^+ + H^+ = H_2\mathbf{L1}^{2+}$	9.40(1)
$H_2\mathbf{L1}^{2+} + H^+ = H_3\mathbf{L1}^{3+}$	9.02(1)
$H_3\mathbf{L1}^{3+} + H^+ = H_4\mathbf{L1}^{4+}$	7.52(2)
$H_4\mathbf{L1}^{4+} + H^+ = H_5\mathbf{L1}^{5+}$	2.59(4)

[a] Values in parentheses are the standard deviations on the last significant figure.

Table 6
Logarithm of the equilibrium constants determined in 0.15 mol dm^{-3} NaCl aqueous solution at 310.1 K for the complexation reactions of **L1** with Cu(II)

Reaction	log *K*
$Cu^{2+} + \mathbf{L1} = Cu\mathbf{L1}^{2+}$	20.90(2)[a]
$Cu^{2+} + \mathbf{L1} + H^+ = Cu(H\mathbf{L1})^{3+}$	29.72(3)
$Cu^{2+} + \mathbf{L1} + 2H^+ = Cu(H_2\mathbf{L1})^{4+}$	33.13(4)
$Cu^{2+} + \mathbf{L1} + 3H^+ = Cu(H_3\mathbf{L1})^{5+}$	36.29(7)
$2Cu^{2+} + \mathbf{L1} = Cu_2\mathbf{L1}^{4+}$	29.59(2)
$2Cu^{2+} + \mathbf{L1} = Cu_2(H_{-1}\mathbf{L1})^{3+} + H^+$	25.03(2)
$2Cu^{2+} + \mathbf{L1} + H_2O = Cu_2(H_{-1}\mathbf{L1})OH^{2+} + 2H^+$	19.09(5)

[a] Values in parentheses are the standard deviations on the last significant figure.

dination of NO with $[Cu_2(H_{-1}\mathbf{L1})OH]^{2+}$ reduces the level of NO in the culture medium of stimulated RAW 264.7 macrophages without any inhibition in the expression of iNOS.

The ligand **L2** (2-((bis(aminoethyl)amino)methyl)phenol) is an analog of **L1** with only one triaminic unit as side arm. Basicity behaviour and ligational properties of this ligand towards Ni(II), Cu(II), Zn(II) [8] and heavy metal ions such Cd(II) and Pb(II) were studied by means of potentiometric measurements in aqueous solution (298.1 K, $I = 0.15$ mol dm^{-3}). The anionic $H_{-1}\mathbf{L2}^-$ species can be obtained in strong alkaline solution; this species behaves as tetraprotic base in the experimental conditions used (Table 7).

Table 7
Protonation constants (log *K*) of **L2** determined by means of potentiometric measurements in 0.15 mol dm^{-3} NaCl aqueous solution at 298.1 K

Reaction	log *K*
$H_{-1}\mathbf{L2}^- + H^+ = \mathbf{L2}$	11.06(1)[a]
$\mathbf{L2} + H^+ = H\mathbf{L2}^+$	9.86(1)
$H\mathbf{L2}^+ + H^+ = H_2\mathbf{L2}^{2+}$	8.46(1)
$H_2\mathbf{L2}^{2+} + H^+ = H_3\mathbf{L2}^{3+}$	2.38(2)

[a] Values in parentheses are the standard deviations on the last significant figure.

L2 forms mono- and dinuclear complexes in aqueous solution with all transition metal ions examined (Table 8). The dinuclear species shows the $[M_2(H_{-1}\mathbf{L2})_2]^{2+}$ stoichiometry, where M = Ni(II), Cu(II), Zn(II), Cd(II) and Pb(II) [9], in which the ligand/metal ratio is 2:2.

The studies revealed that two mononuclear $[M(H_{-1}\mathbf{L2})]^+$ species self-assemble, giving the dinuclear complexes, which can be easily isolated as perchlorate salt from the aqueous solution due to their low solubility. This behaviour is ascribed to the fact that **L2** does not fulfil the coordination requirement of the ion in the mononuclear species and to the capacity of the phenolic oxygen, as phenolate, to bridge two metal ions.

Table 8
Logarithm of the equilibrium constants determined in 0.15 mol dm^{-3} NMe_4Cl at 298.1 K for the complexation reactions of **L2** with Co(II), Ni(II), Cu(II) and Zn(II) ions

Reaction	log *K*				
	Ni(II)	Cu(II)	Zn(II)	Cd(II)	Pb(II)
$M^{2+} + H_{-1}\mathbf{L2}^- = M(H_{-1}\mathbf{L2})^+$	14.80(1)[a]	19.12(1)	15.07(2)	11.16(1)	10.86(1)
$M^{2+} + H_{-1}\mathbf{L2}^- + H^+ = M(\mathbf{L2})^{2+}$	20.80(3)	23.54(1)		16.94(5)	17.68(2)
$M^{2+} + H_{-1}\mathbf{L2}^- + 2H^+ = M(H\mathbf{L2})^{3+}$		27.62(7)			
$M^{2+} + H_{-1}\mathbf{L2}^- + H_2O = M(H_{-1}\mathbf{L2})OH + H^+$	3.56(3)	8.76(2)	4.39(2)	0.48(2)	0.08(2)
$M^{2+} + H_{-1}\mathbf{L2}^- + 2H_2O = M(H_{-1}\mathbf{L2})(OH)_2^- + 2H^+$		−1.78(3)			
$2M^{2+} + 2H_{-1}\mathbf{L2}^- = M_2(H_{-1}\mathbf{L2})_2^{2+}$	31.25(5)	40.96(3)	32.23(4)		
$2M^{2+} + 2H_{-1}\mathbf{L2}^- + H_2O = M_2(H_{-1}\mathbf{L2})_2OH^+ + H^+$		31.70(3)			

[a] Values in parentheses are the standard deviations on the last significant figure.

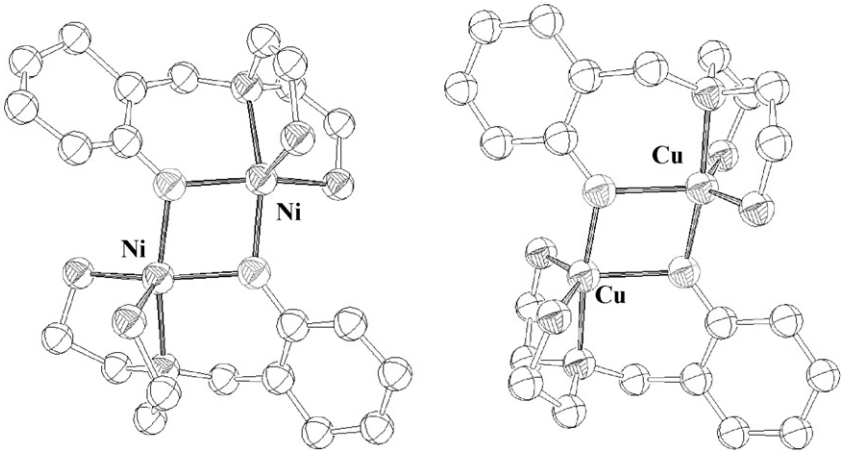

Fig. 4. ORTEP view of the complex cations $[Ni_2(H_{-1}\mathbf{L2})_2]^{2+}$ and $[Cu_2(H_{-1}\mathbf{L2})_2]^{2+}$.

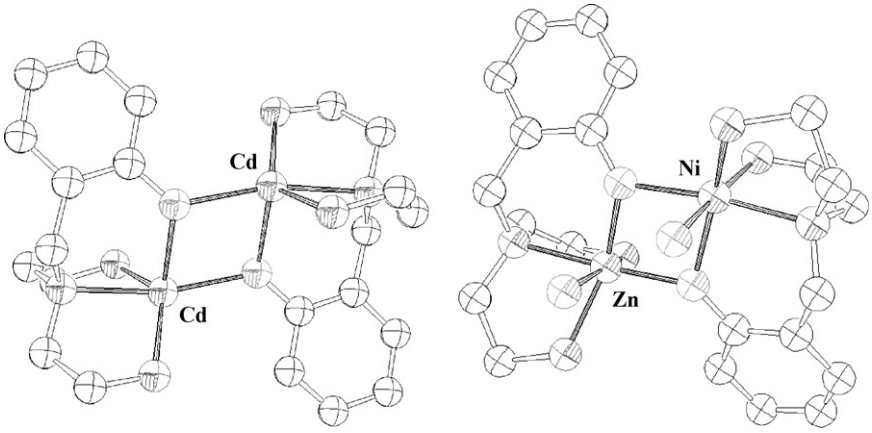

Fig. 5. ORTEP view of the complex cation $[Cd_2(H_{-1}\mathbf{L2})_2]^{2+}$ and $[ZnNi(H_{-1}\mathbf{L2})_2]^{2+}$.

All dinuclear species were characterized by determining their crystal structures, which showed similar coordination patterns. All metal ions are substantially coordinated by three amine functions and two oxygen atoms of the phenolate moieties (see Fig. 4). The two metals in the dinuclear complexes are at short distance, in all the dinuclear complexes the M(II)–M(II) separation is in the range of 3.023–3.446 Å, interacting together as shown by magnetic measurements performed with Ni(II) and Cu(II) complexes, which revealed an antiferromagnetic coupling between the two metal ions.

The $[Cu_2(H_{-1}\mathbf{L2})_2]^{2+}$ cation has a Cu(II)–Cu(II) separation of 3.088 Å at $T > 100$ K and of 3.139 Å at $T < 100$ K, and shows a phase transition occurring by the temperature between 90 and 100 K; the characterization of the compounds existing at different temperatures was investigated using X-ray single-crystal diffraction, EPR, and magnetic measurements. By mixing the homodinuclear $[Zn_2(H_{-1}\mathbf{L2})_2]^{2+}$ (Zn(II)–Zn(II) distance = 3.140 Å) and $[Ni_2(H_{-1}\mathbf{L2})_2]^{2+}$ (Ni(II)–Ni(II) distance = 3.044 Å) complexes, the heterodinuclear $[ZnNi(H_{-1}\mathbf{L2})_2]^{2+}$, with a Zn(II)–Ni(II) separation of 3.023 Å, was obtained (Fig. 5) [10]. The authors also reported the structure of Cd(II) dinuclear complex $[Cd_2(H_{-1}\mathbf{L2})_2]^{2+}$, in which the Cd(II)–Cd(II) separation is of 3.446 Å (Fig. 5).

Although ligand **L3** (1-(2-hydroxybenzyl)-1,5-diazacyclooctane) could not be considered as a pure acyclic ligand, it has been inserted in this section because mesocyclic amine ligands and their derivatives could be considered as "bridging" or borderline molecules between the two major class of ligands called acyclic and macrocyclic ligands. Ligand **L3** is a small molecule formed by a phenolic pendant side arm attached to the 1,5-diazacyclooctane; this singular combination gives rise to penta-coordinated complexes [11] $[Co(H_{-1}\mathbf{L3})Cl]_2$ as that depicted in Fig. 6.

The *boat*/*chair* conformation adopted by the 1,5-diazacyclooctane (DACO) inhibits the axial coordination at the metal centre, preventing the formation of hexa-coordinated complexes. In Fig. 6 it can be observed as the phenol disposes itself in a bridged disposition.

Another ligand bearing saturated aminic arms is **L4** that forms dinuclear Mn(II) complexes. The discussion of its behaviour will be done below.

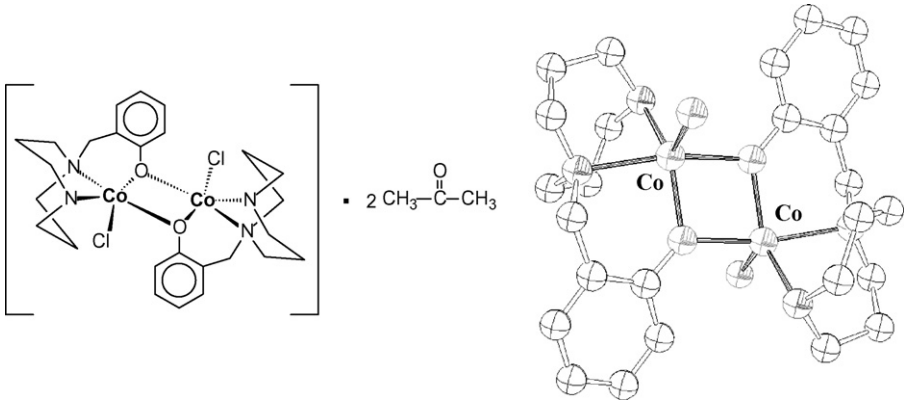

Fig. 6. Schematic and ORTEP view of the complex $[Co(H_{-1}\mathbf{L3})Cl]_2$.

2.1.1.2. Phenolic ligands bearing imine and pyridine side-arms.

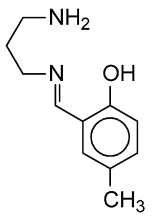

L5

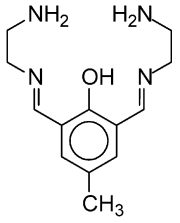

L6

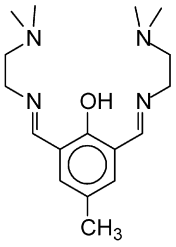

L7

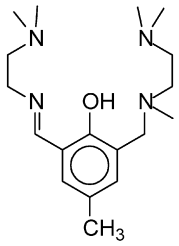

L8

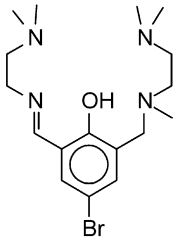

L9

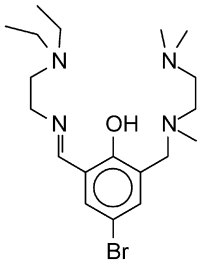

L10

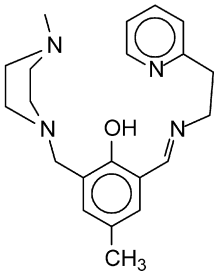

L11

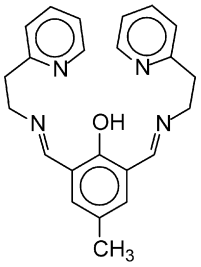

L12

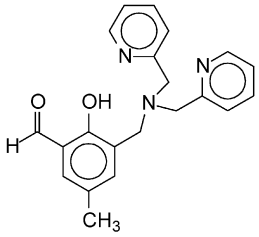

L13

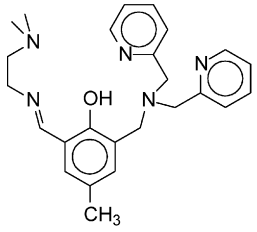

L14

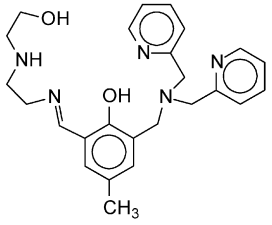

L15

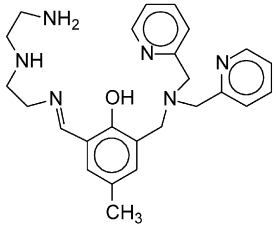

L16

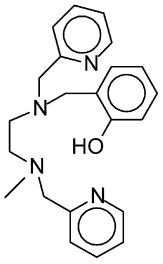

L17

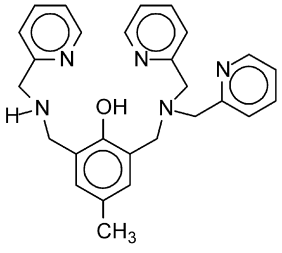

L18

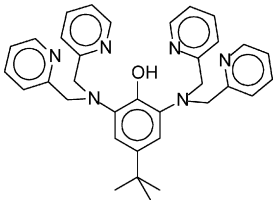

L19

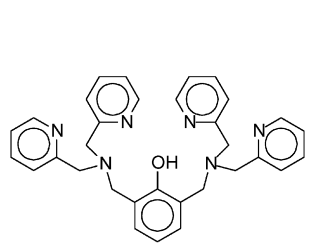

L20

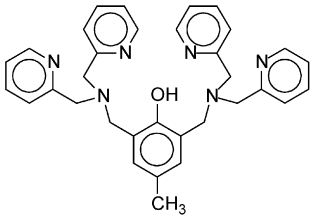

L21

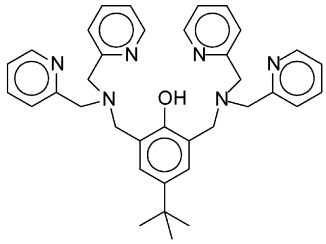

L22

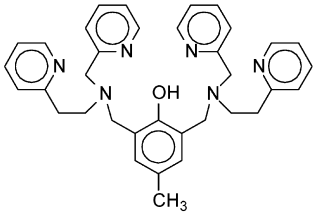

L23

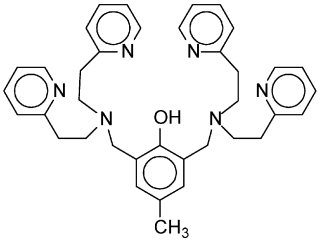

L24

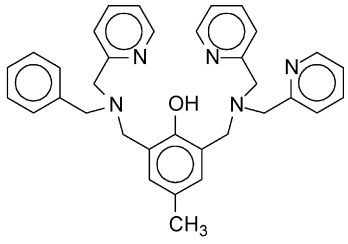

L25

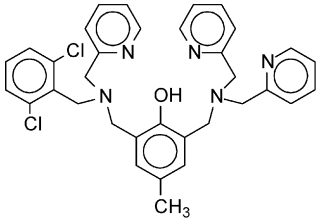

L26

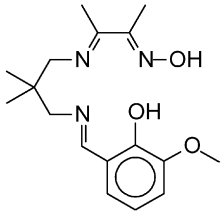

L27

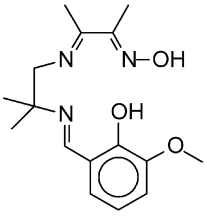

L28

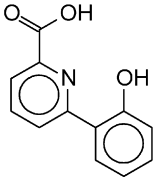

L29

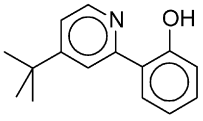

L30

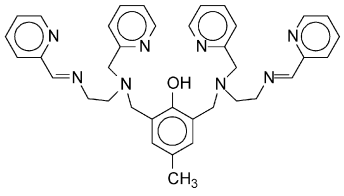

L31

The ligand **L5** (*N*-(3-aminopropyl)salicylaldimine) forms dinuclear Ni(II) complex $[Ni_2(H_{-1}\mathbf{L5})_2(H_2O)(NCS)_2]$, in which the metal ions are bridged by one water molecule and two μ-phenolate ions, and a thiocyanato-bridged dimeric Cu(II) complex [12] $[Cu(H_{-1}\mathbf{L5})(NCS)]_2$. The complexes were characterized by IR and UV/vis spectroscopy, cyclic voltammetry and single-crystal X-ray diffraction studies. The structure of $[Ni_2(H_{-1}\mathbf{L5})_2(H_2O)(NCS)_2]$ consists of dinuclear units with crystallographic C2 symmetry in which each Ni(II) atom is in a distorted octahedral environment, the Ni(II)–Ni(II) distance is 2.953 Å. The structure of $[Cu(H_{-1}\mathbf{L5})(NCS)]_2$ consists of dinuclear units bridged asymmetrically by di-$\mu_{1,3}$-NCS ions with Cu(II)–Cu(II) distance of 5.863 Å; each Cu(II) ion is in a square-pyramidal environment. Variable-temperature magnetic susceptibility studies indicate dominant ferromagnetic exchange coupling in complex $[Ni_2(H_{-1}\mathbf{L5})_2(H_2O)(NCS)_2]$ with $J = 3.1\,cm^{-1}$, whereas complex $[Cu(H_{-1}\mathbf{L5})(NCS)]_2$ exhibits weak antiferromagnetic coupling between the Cu(II) centres with $J = -1.7\,cm^{-1}$.

The ligand **L6** (2,6-bis[*N*-(2-aminoethy)iminomethyl]-4-methylphenol) forms dinuclear complexes with Cu(II) ions [13] (distance Cu–Cu = 3.032 Å) which is able to coordinate three azide anions. In the neutral $[Cu_2(H_{-1}\mathbf{L6})(N_3)_2(\mu_{1,1}\text{-}N_3)(H_2O)]$ species the two Cu(II) ions are connected by two different kind of bridges, one it is an endogenous phenoxo bridge provided by the phenolate group and the other is an exogenous azido bridge.

Sakijama, Okawa and Fenton's groups investigated the coordination properties of the N_4O-type ligand series **L9** (4-bromo-2-{[(dimethylaminoethyl)metylamino]methyl}-6-[2-(dimethylamino)-ethyliminomethyl]phenol), **L4** (2,6-bis{[*N*-(dimethylaminoethyl)-*N*-metyl]aminomethyl}4-methylphenol) and **L10** (4-bromo-2-{[(dimethylaminoethyl)metylamino]methyl}-6-[2-(diethylamino)ethyliminomethyl]phenol) towards Mn(II) ions. **L9** and **L10** are asymmetric phenol-based dinucleating ligands with amino and imino chelating arms that formed dinuclear Mn(II) complexes $[Mn_2(H_{-1}\mathbf{L9})(OOCR)_2(NCS)]$ and $[Mn_2(H_{-1}\mathbf{L10})(OOCR)_2(NCS)]$, where R = Me or Ph [14]. The asymmetric ligands provide different co-ordination geometries about the two manganese ions, the Mn(II)–Mn(II) separation in

Table 9
Apparent rate constants for disproportionation of H_2O_2 by dinuclear complexes $[Mn_2(H_{-1}\mathbf{L4})(p\text{-}XC_6H_4COO)_2(NCS)(MeOH)]2H_2O_2 \rightarrow 2H_2O + O_2 - d[H_2O_2]/dt = k'[H_2O_2]$

X	k' (min^{-1})
NO_2	0.260
Cl	0.100
Me	0.069
H	0.049

$[Mn_2(H_{-1}\mathbf{L10})(OOCMe)_2(NCS)]$ was of 3.376 Å. The geometry of Mn at the imine site is a distorted trigonal bipyramidal with the amine nitrogen and the two acetate oxygen atoms in the basal plane and the phenolic oxygen and the terminal nitrogen at the axial sites. The geometry of the Mn at the amine sites is distorted octahedral involving also the nitrogen of the isothiocyanato group. Cyclic voltammetry studies revealed three *quasi* reversible red-ox couples assignable to the stepwise Mn(II)Mn(II) → Mn(II)Mn(III) → Mn(III)Mn(III) → Mn(III) Mn(IV). The symmetric ligand **L4** formed complexes $[Mn_2(H_{-1}\mathbf{L4})(p\text{-}XC_6H_4COO)_2(NCS)(MeOH)]$ (X = H, Cl, Me or NO_2). The isothiocyanato ion is co-ordinated to one of the Mn(II) ions and the methanol molecule to the other, providing distorted-octahedral geometries around each manganese.

All the complexes show a catalase-like activity in disproportionating H_2O_2 into O_2 and H_2O, with rates which follow he trend $NO_2 > Cl > Me > H$ (Table 9). The authors showed a hypothesis for the catalytic cycle that underlines the crucial presence of oxomanganese(IV) intermediates (Scheme 1) [15].

L7 (2,6-bis{*N*-[2-(dimethylamino)ethyl]iminomethyl}-4-methylphenol), **L8** (2-{[(dimethylamino-ethyl)metyl-amino] methyl}-6-[2-(dimethylamino)ethyliminomethyl]-4-methylphenol) and **L2**, were used to prepare dinuclear Ni(II) complexes [16] $[Ni_2(H_{-1}\mathbf{L7})(AcO)(NCS)_2(MeOH)]$, $[Ni_2(H_{-1}\mathbf{L7})(AcO)_2(MeOH)]BPh_4$ (Ni(II)–Ni(II) distance = 3.311 Å), $[Ni_2(H_{-1}\mathbf{L9})(AcO)(NCS)_2(MeOH)]$ (Ni(II)–Ni(II) distance = 2.993 Å), $[Ni_2(H_{-1}\mathbf{L9})(AcO)_2]BPh_4$ (Ni(II)–Ni(II) distance = 3.254 Å), $[Ni_2(H_{-1}\mathbf{L9})(NCS)_3(MeOH)]$ (Ni(II)–Ni(II) distance = 3.142 Å, Fig. 7), $[Ni_2(H_{-1}\mathbf{L7})(OH)(py)(H_2O)](ClO_4)_2$ (Ni(II)–Ni(II) distance = 2.967 Å), $[Ni_2(H_{-1}\mathbf{L8})(OH)(MeOH)(H_2O)](ClO_4)_2$ and $[Ni_2(H_{-1}\mathbf{L8})(OH)(DMF)_2](ClO_4)_2$ (Ni(II)–Ni(II) distance = 2.992 Å). These complexes could be interesting to mimic the activity of urease. Urease is a Ni(II) dependant enzyme that catalyzes the hydrolysis of urea to ammonium carbamate. In order to evaluate the relevance of these dinuclear species as model for urease, all the complexes were examined regarding their ability to bind urea. The $[Ni_2(H_{-1}\mathbf{L9})(AcO)_2(urea)]BPh_4$, $[Ni_2(H_{-1}\mathbf{L9})(NCS)_3(urea)]$ (Fig. 7), $[Ni_2(H_{-1}\mathbf{L7})(OH)(urea)(H_2O)](ClO_4)_2$ (Ni(II)–Ni(II) distance = 2.977 Å) and $[Ni_2(H_{-1}\mathbf{L8})(OH)(urea)(H_2O)](ClO_4)_2$ (Ni(II)–Ni(II) distance = 2.992 Å) urea adducts were obtained [17].

The ligands **L7**, **L9**, **L12** (2,6-bis{2-[(2-pyridyl)ethyl]iminomethyl}-4-methylphenol) and **L14** (2-[*N*,*N*-bis(2-pyridylmethyl)aminomethyl]-6-{*N*-[2-(dimethylamino)ethyl]iminomethyl}-4-methylphenol) formed dinuclear Zn(II) complexes [18]: $[Zn_2(H_{-1}\mathbf{L7})(AcO)_2]PF_6$, $[Zn_2(H_{-1}\mathbf{L7})(NCS)_3]$, $[Zn_2(H_{-1}\mathbf{L9})(AcO)_2]PF_6$, $[Zn_2(H_{-1}\mathbf{L9})(NCS)_3]$, $[Zn_2(H_{-1}\mathbf{L12})(AcO)_2]PF_6$, $[Zn_2(H_{-1}\mathbf{L12})(NCS)_3]$, $[Zn_2(H_{-1}\mathbf{L14})(AcO)_2]ClO_4$, $[Zn_2(H_{-1}\mathbf{L14})(AcO)(NCS)_2]$ and $[Zn_2(H_{-1}\mathbf{L14})(NCS)_3]$. X-ray analysis revealed the presence of a μ-phenolato-dizinc(II) core (Fig. 8).

Most of these diacetato complexes are stable in aqueous solution. Hydrolytic activities of the complexes towards tris(*p*-nitrophenyl)phosphate (TNP) were studied in aqueous DMF by UV–visible spectroscopic and ^{31}P NMR methods. Complexes $[Zn_2(H_{-1}\mathbf{L7})(AcO)_2]PF_6$, $[Zn_2(H_{-1}\mathbf{L9})(AcO)_2]PF_6$ and $[Zn_2(H_{-1}\mathbf{L12})(AcO)_2]PF_6$ have an activity to hydrolyze TNP into bis(*p*-nitrophenyl) hydrogenphosphate (HBNP) in aqueous DMF. In contrast, $[Zn_2(H_{-1}\mathbf{L14})(AcO)_2]ClO_4$ showed little hydrolytic activity towards TNP in aqueous DMF (Scheme 2) [19].

The pyridinic-phenolic ligands **L23** (2,6-bis{[(2-(2-pyridyl)ethyl)(2-pyridylmethyl)amino]methyl}-4-methylphenol), **L24**

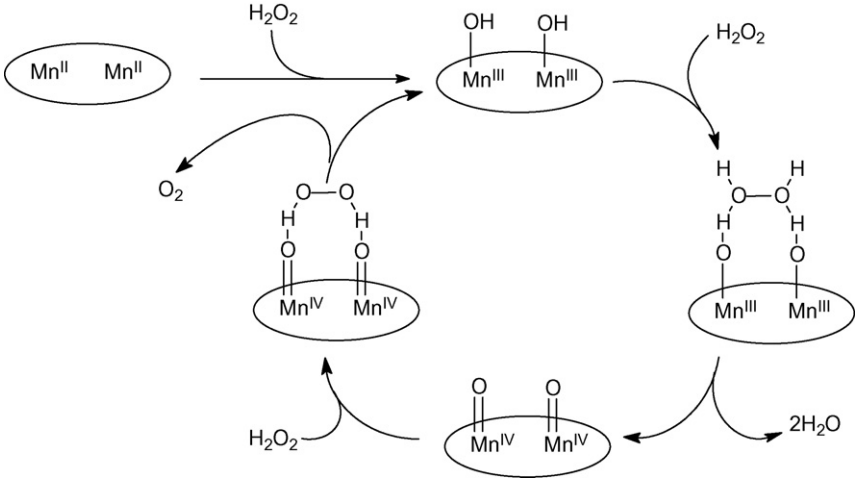

Scheme 1. Proposed mechanism for the disproportionation of hydrogen peroxide by Mn(II) dinuclear complexes ($2\ H_2O_2 \rightarrow 2H_2O + O_2$).

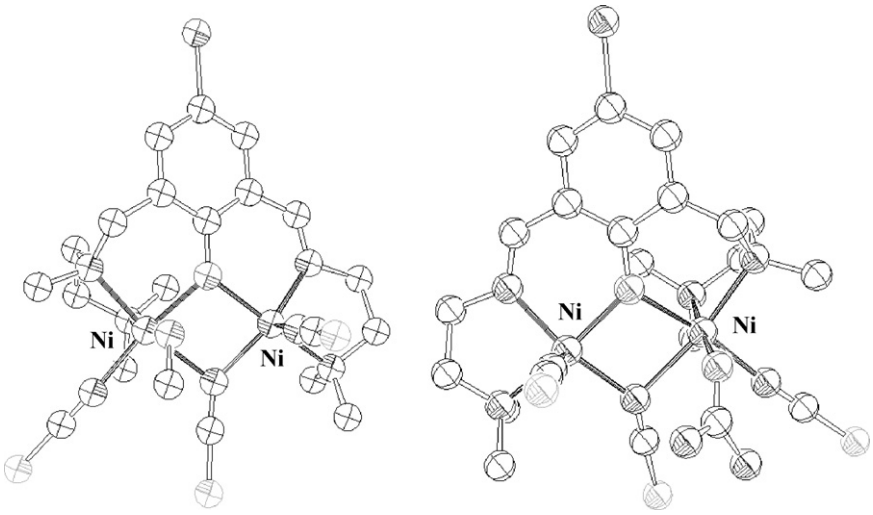

Fig. 7. ORTEP view of the complex cations $[Ni_2(H_{-1}\mathbf{L9})(NCS)_3(MeOH)]$ and $[Ni_2(H_{-1}\mathbf{L9})(NCS)_3(urea)]$.

(2,6-bis{[(*N*,*N*-bis(2-(2-pyridyl)ethyl)amino]methyl}-4-methylphenol) and **L21** (2,6-bis{[(*N*,*N*-bis(2-pyridylmethyl) amino]methyl}-4-methylphenol) were investigated towards Mn(II) or Mn(III) ions [20]. The ligand **L23** is able to form dinuclear Mn(II) complexes. The $[Mn_2(II,II)(H_{-1}\mathbf{L23})(OAc)_2]ClO_4$ species, after electrolytic oxidation at 0.7 V (vs. Ag/AgCl), produces the mixed valence complex $[Mn_2(II,III)(H_{-1}\mathbf{L23})(OAc)_2](ClO_4)_2$. X-ray crystallography structures show that both $[Mn_2(II,II)(H_{-1}\mathbf{L23})(OAc)_2]ClO_4$ and $[Mn_2(II,III)(H_{-1}\mathbf{L23})(OAc)_2](ClO_4)_2$ are dinuclear complexes in which the two Mn(II) ions are each in distorted octahedral coordination environments bridged by the phenoxo oxygen atom and two acetate ions. The structural changes that occur after the oxidation suggest an extended π-bonding system involving the phenoxo ring $C–O_{phenoxo}–Mn(II)–N_{pyridyl}$ chain. As $[Mn_2(II,II)(H_{-1}\mathbf{L23})(OAc)_2]ClO_4$ (Mn(II)–Mn(II) distance = 3.469 Å) is oxidized to $[Mn_2(II,III)(H_{-1}\mathbf{L23})(OAc)_2](ClO_4)_2$ (Mn(II)–Mn(III) distance = 3.486 Å), the rearrangement in the coordination sphere resulting from the oxidation of one Mn(II) ion to Mn(III) is transmitted via the bridging Mn–O phenoxo bonds and causes structural changes that make the site of the second Mn ion unfitting for the Mn(III) state and hence unstable to reduction. In fact, after the electrolytic oxidation of $[Mn_2(II,III)(H_{-1}\mathbf{L23})(OAc)_2](ClO_4)_2$ in MeCN at 1.20 V, the starting complex is recovered, showing the instability of the $Mn_2(III,III)$ state. Magnetic susceptibility measurements of $[Mn_2(II,II)(H_{-1}\mathbf{L23})(OAc)_2]ClO_4$ and $[Mn_2(II,III)(H_{-1}\mathbf{L23})(OAc)_2](ClO_4)_2$ at 1.8–300 K show the weak antiferromagnetic coupling between the two Mn ions in each dinuclear complex, which is commonly observed among similar phenoxo- and bis-1,3-carboxylato-bridged dinuclear $Mn_2(II,II)$ and $Mn_2(II,III)$ complexes.

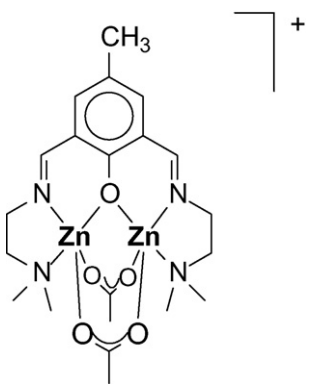

Fig. 8. Structure of the complex cation $[Zn_2(H_{-1}\mathbf{L7})(AcO)_2]^+$.

The dinucleating ligand **L11** (2-[(2-pyrid-2-ylethyl) iminomethyl]-6-[(4-methylpiperazin-1-yl)methyl]phenol) formed asymmetrical dinuclear Cu(II) complex $[Cu_2(H_{-1}\mathbf{L11})(OAc)_2](ClO_4)$. The crystal structure establishes a dinuclear copper core with distinct copper sites [21]. One of the Cu(II) ions is coordinated by two sp^3 nitrogen atoms whereas the other Cu(II) ion is coordinated by two sp^2 nitrogen atoms. The two Cu(II) ions are bridged by a phenoxo group, by a syn–syn bidentate acetato bridge, and by a monodentate acetato bridge giving a Cu–Cu distance of 3.029 Å. The copper centres are weakly antiferromagnetically coupled with $2J = -15\,cm^{-1}$. This weak antiferromagnetic coupling is reflected in the large isotropic shifts for the ligand protons in the ^1H NMR spectrum of $[Cu_2(H_{-1}\mathbf{L11})(OAc)_2](ClO_4)$. The complex formation was studied by microcalorimetric and UV–visible titrations These techniques unambiguously establish the stepwise complexation behaviour of the ligand: asymmetrical dinuclear complex $[Cu_2(H_{-1}\mathbf{L11})(OAc)_2](ClO_4)$ is formed via the initial formation of a mononuclear Cu(II) complex. The enthalpy of formation of the first complexation step is $\Delta H = -8.4$ kcal/mol ($K = 1.8 \times 10^8$); for the second step a value of $\Delta H = -1.9$ kcal/mol ($K = 1.1 \times 10^5$) was obtained using microcalorimetry.

The ligand **L22** (2,6-bis{[bis(2-pyridylmethyl) amino]methyl}-4-*tert*-butylphenol) was able to form a series of mixed-valent iron and mixed-metal Fe(III)–M(II) (M = Fe, Zn, Cu, Ni or Co) complexes, in which both

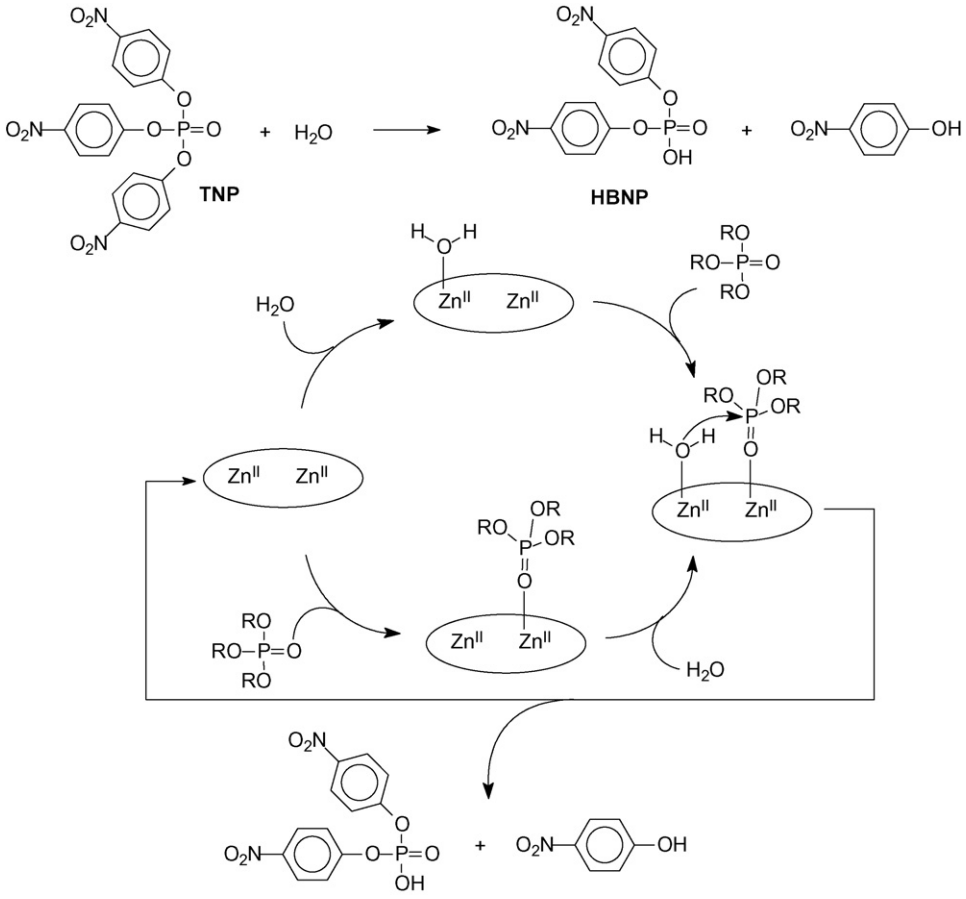

Scheme 2. Proposed mechanism of TNP hydrolysis by Zn(II) dinuclear complexes (R = O_2N-*p*-C_6H_4-OH).

exogenous bidentate bridging groups and different terminal ligands bound to each different metal ion at the exogenous site were identified [22]. The mixed-valence complex $[Fe_2(III,II)(H_{-1}\mathbf{L22})(F)_2(H_2O)_2](BF_4)_2$ is a rare example of a dimetallic complex of a single-atom hinged acyclic dinucleating ligand with a non-bridged arrangement at the exogenous bridging site. The Fe(II) and Fe(III) atoms are bridged asymmetrically by the phenolic oxygen atom of $H_{-1}\mathbf{L22}$ with a Fe(III)–Fe(II) distance of 3.726 Å. The two terminal fluoride ions are bound to the Fe(III) ion and strongly hydrogen bonded to two water molecules bound to the adjacent Fe(II) ion. This complex may model the mode in which fluoride ions bind the active site of the purple acid phosphatases (PAPs) thereby inhibiting the activity of these enzymes. Tetrahedral oxo anions are known also to inhibit PAPs, and to mimic this inhibition a Fe(III)–Zn(II) complex $[FeZn(H_{-1}\mathbf{L22})(MoO_4)_2]$ incorporating molybdate bridging groups was prepared. The Fe(III)–Zn(II) distance is 3.819 Å. A series of acetate-bridged complexes were prepared by the novel method of diffusing ethyl acetate or iso-propyl acetate into mixtures of **L22** and iron perchlorate in the presence and absence of second type of metal ion. The acetate bridging groups are the result of the hydrolysis of the alkyl acetate. These complexes have the general formulation $[FeM(H_{-1}\mathbf{L22})(CH_3CO_2)_2](ClO_4)_2$, where M = Zn, Cu, Ni or Co. Asymmetrical bridging by the hinging phenolate group is evident in the bis(molybdate)-bridged Fe(III)–Zn(II) complex $[FeZn(H_{-1}\mathbf{L22})(MoO_4)_2]$ and the bis(acetate)-bridged Fe(III)–Cu(II) complex $[FeCu(H_{-1}\mathbf{L22})(CH_3CO_2)_2](ClO_4)_2$, however it is significantly less pronounced compared with the non-bridged fluoride containing Fe(III)–Fe(II) complex. While the fluoride and molybdate complexes may model aspects of the binding of these ions in inhibited PAPs, the generation of acetate complexes from the hydrolysis of alkyl esters may indeed model part of the reactivity of PAPs.

The ligand **L13** (3-[[bis(2-pyridinylmethyl)amino]methyl]-2-hydroxy-5-methylbenzaldeide), which contains a tridentate amino arm and a weak donor aldehyde group at the two and six positions of the phenol ring, respectively, formed dinuclear complexes $[Co_2(H_{-1}\mathbf{L13})_2](ClO_4)_2$, $[Co_2(H_{-1}\mathbf{L13})_2](BF_4)_2$, $[Mn_2(H_{-1}\mathbf{L13})_2](ClO_4)_2$. The two metal ions are doubly bridged by two deprotonated cresolate moieties and the coordination environment around the metal ions is completed in a very distorted octahedron by three N donor atoms from the pendant amino arm and the O atom of the aldehyde group (Fig. 9) [23]. In the dinuclear Mn(II) complex, the Mn(II)–Mn(II) separation is 3.401 Å.

Anxolabéhère-Mallart and Blondin reported the ligand **L17** (*N*,*N*′-bis(2-pyridylmethyl)-*N*-(2-hydroxybenzyl)-

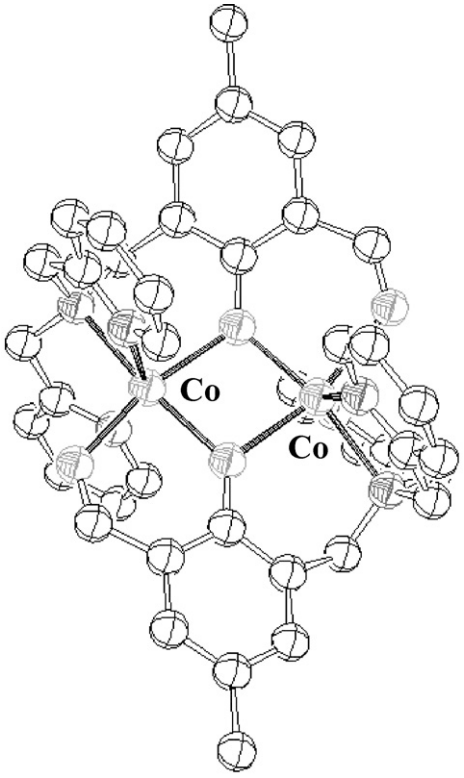

Fig. 9. ORTEP view of the complex cation $[Co_2(H_{-1}\mathbf{L13})_2]^{2+}$.

N′-methylethane-1,2-diamine) that gives dinuclear phenolato-bridged complex $[Mn(II,II)_2(H_{-1}\mathbf{L17})_2](ClO4)_2$, characterized by X-ray crystallography [24]. Cyclic voltammetry of $[Mn(II,II)_2(H_{-1}\mathbf{L17})_2](ClO4)_2$ exhibits two irreversible oxidation waves at $E_1 = 0.89$ V and $E_2 = 1.02$ V, accompanied on the reverse scan by an ill-defined cathodic wave at $E_{1'} = 0.56$ V (all measured versus the SCE). After chemical oxidation with *t*BuOOH at 293.1 K, $[Mn_2(II,II)(H_{-1}\mathbf{L17})_2](ClO4)_2$ is transformed into the mono-μ-oxo species $[Mn_2(III,III)(H_{-1}\mathbf{L17})_2(\mu\text{-}O)]^{2+}$, in which one of the aromatic rings of the ligand is decoordinated. The UV/vis spectrum of $[Mn_2(III,III)(H_{-1}\mathbf{L17})_2(\mu\text{-}O)]^{2+}$ displays a large absorption band at 507 nm, which is attributed to a phenolate → Mn(III) charge-transfer transition. The cyclovoltammogram of $[Mn_2(III,III)(H_{-1}\mathbf{L17})(\mu\text{-}O)]^{2+}$ exhibits two reversible oxidation waves, at 0.65 and 1.16 V vs. the SCE, corresponding to the Mn(III)Mn(III) → Mn(III)Mn(IV) and Mn(III)Mn(IV) → Mn(IV)Mn(IV) oxidation processes, respectively. The mono-electron electrochemical oxidation of $[Mn_2(III,III)(H_{-1}\mathbf{L17})_2(\mu\text{-}O)]^{2+}$ leads to the mono-μ-oxo mixed-valent species $[Mn_2(III,IV)(H_{-1}\mathbf{L17})_2(\mu\text{-}O)]^{3+}$. The UV/vis spectrum of $[Mn_2(III,IV)(H_{-1}\mathbf{L17})_2(\mu\text{-}O)]^{3+}$ exhibits one large band at 643 nm, which is attributed to the phenolate → Mn(IV) charge-transfer transition. $[Mn_2(III,IV)(H_{-1}\mathbf{L17})_2(\mu\text{-}O)]^{3+}$ can also be obtained by the direct electrochemical oxidation of $[Mn_2(II,II)(H_{-1}\mathbf{L17})_2](ClO_4)_2$ in the presence of an external base.

Dinuclear Ni(II) complex $[Ni_2(H_{-1}\mathbf{L18})(OAc)_2(H_2O)]ClO_4$, with the unsymetrical N_5O donor ligand **L18** (2-{[bis (2-pyridylmethyl)amino]methyl}-4-methyl-6-{[2-pyridylmethylamino]methyl}phenol) was synthesized and characterized by Greatti and co-workers. In this complex both Ni(II) ions have a distorted octahedral geometry [25]. The Ni(II) centres are endogenously bridged by the phenolic O atom of the deprotonated ligand and also bridged by the two acetate groups as exogenous bridge. A H_2O molecule as terminal ligand is coordinated to a Ni(II) ion. As other dinuclear Ni(II) complexes, this complex can be used as mimic of urease, whereas Ni(II)–Ni(II) separation is of 3.422 Å, slightly shorter than that observed in *Klebsiella aerogenes* urease (3.5 Å) and *Bacillus Pasteuri* urease (3.7 Å).

The unsymmetrical ligand **L25** (2-((bis(2-pyridylmethyl) amino)methyl)-6-(((2-pyridylmethyl)benzylamino)methyl)-4-methylphenol) and its 2,6-dichlorobenzyl analogue **L26** (2-((bis(2-pyridylmethyl)amino)methyl)-6-(((2-pyridylmethyl) (3,5-dichlorobenzyl)amino)methyl)-4-methylphenol), afford the mixed valence diiron(II,III) complexes $[Fe_2(II,III)(H_{-1}\mathbf{L25})(mpdp)(H_2O)](ClO_4)_2$ and $[Fe_2(II,III)(H_{-1}\mathbf{L26})(mpdp)(CH_3OH)](ClO_4)_2$, when they react with $Fe(ClO_4)_2$ in the presence of disodium *m*-phenylenedipropionate (Na_2mpdp) followed by exposure to air [26]. The complex $[Fe_2(II,III)(H_{-1}\mathbf{L25})(mpdp)(H_2O)](ClO_4)_2$ was characterized by X-ray crystallography. After dissolution in acetonitrile the terminal ligand on the Fe(II) site in the cation $[Fe_2(II,III)(H_{-1}\mathbf{L25})(mpdp)(H_2O)]^{2+}$ is replaced by a solvent molecule. The acetonitrile-water exchange was investigated by various spectroscopic techniques (UV/vis, NMR, Mossbauer) and electrochemical studies. Exhaustive electrolysis of a solution of $[Fe_2(II,III)(H_{-1}\mathbf{L25})(mpdp)(H_2O)]^{2+}$ shows that the aqua diferric species $[Fe_2(III,III)(H_{-1}\mathbf{L25})(mpdp)(H_2O)]^{3+}$ is not stable and undergoes a chemical reaction which can be partly reversed by reduction to the mixed-valent state. This and other electrochemical observations suggest that after oxidation of the diiron center to the diferric state the aqua ligand is deprotonated to a hydroxo. This hypothesis is supported by Mossbauer spectroscopy. The authors illustrate the drastic effects of aqua ligand exchange and deprotonation on the electronic structure and redox potentials of diiron centres.

The asymmetrical ligands **L15** (2-[*N*,*N*-bis(2-pyridinilmethyl)aminomethyl]-6-{*N*-[*N*′-(2-hydroxyethyl)aminoethyl] iminomethyl}-4-methylphenol) and **L16** (2-[*N*,*N*-bis (2- pyridinilmethyl) aminomethyl] - 6 - {*N* - [*N*′ -(2-aminoethyl) aminoethyl]iminomethyl}-4-methylphenol), derived from phenol and bearing a terdentate linear arm and a terdentate dipodal arm, give two dinuclear Ni(II) complexes [27], $Ni_2(H_{-1}\mathbf{L15})(OAc)_2](BF_4)$ and $[Ni_2(H_{-1}\mathbf{L16})(OAc)(NCS)_2]$ (Fig. 10). The binding of the terminal donor atoms of the terdentate linear arm appears to be dependent on the nature of the accompanying counteranion. In the complex $[Ni_2(H_{-1}\mathbf{L15})(OAc)_2](BF_4)$, in the presence of the non-coordinating tetrafluoroborate anion, the terminal alcool function is coordinated, whereas in $[Ni_2(H_{-1}\mathbf{L16})(OAc)(NCS)_2]$, in the presence of added isothiocyanate ion, the terminal amine group is not coordinated.

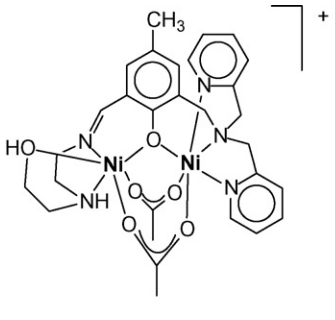

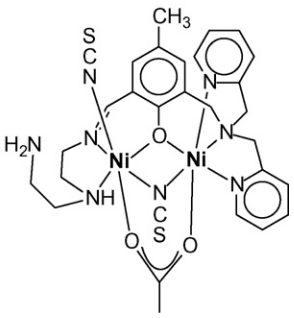

Fig. 10. Structure of the complexes $[Ni_2(H_{-1}\mathbf{L15})(OAc)_2]^+$ and $Ni_2(H_{-1}\mathbf{L16})(OAc)(NCS)_2]$.

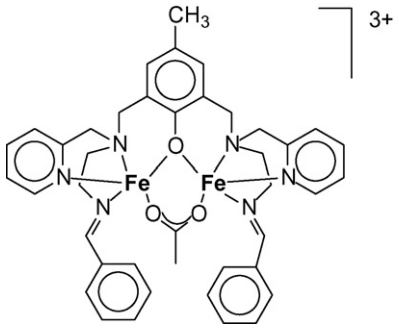

Fig. 12. Structure of the cation complex $[Fe_2(II,III)(H_{-1}\mathbf{L31})(OAc)]^{3+}$.

L20 (2,6-bis{[bis(2-pyridylmethyl)amino]methyl}phenol) forms dinuclear Cu(II) complexes $[Cu_2(H_{-1}\mathbf{L20})(\mu\text{-}O_2)]^+$ reacting with SO_2, CO_2, H^+, phenols, $ArC(O)^+$, PPh_3, and PhMgBr to form sulphate Cu(II) complexes, carbonato-dicopper(II) compounds (via peroxy-carbonato intermediates), to produce H_2O_2 (from excess H^+ or phenols), to form acylperoxo complexes with ArC(O)Cl, to liberate O_2 by addition of PPh_3, and oxygenating PhMgBr ($PhOH:Ph_2 = 3:1$) respectively [28]. By the bound dioxygen, ligand acts as a base or nucleophile towards several substrates, while the behaviour of $[Cu_2(H_{-1}\mathbf{L20})(\mu\text{-}O_2)]^+$ is more typical of early transition metal peroxo complexes.

Costes J. prepared two original heterodinuclear Cu(II)–Gd(III) complexes from polydentate asymmetrical Schiff base phenol oxime ligands **L27** (1-hydroxy-9-(2-hydroxy-3-methoxyphenyl)-2,3,6,6-tetramethyl-1,4,8-triazanona-1,3,8-triene) and **L28** (1-hydroxy-8-(2-hydroxy-3-methoxylphenyl)-2,3,6,6-tetramethyl-1,4,7-triazaotta-1,3,7-triene), that differ by the length of the diamino chain [29]. The complexes have stoichiometry $[CuGd(H_{-2}\mathbf{L27})](NO_3)_3$ (Cu(II)–Gd(III) distance = 3.648 Å) and $[CuGd(H_{-2}\mathbf{L28})](NO_3)_3$ (Cu(II)–Gd(III) distance = 3.621 Å, Fig. 11).

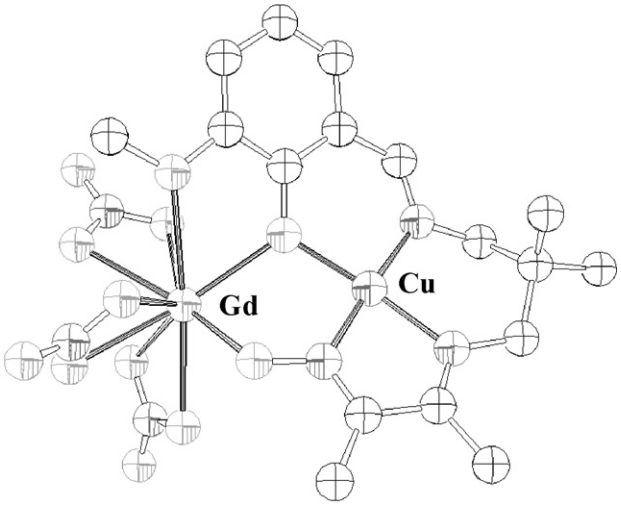

Fig. 11. ORTEP view of the complex $[CuGd(H_{-2}\mathbf{L27})](NO_3)_3]$.

The structural studies show that in both complexes the Cu(II) and Gd(III) ions are doubly bridged by a phenolate oxygen atom and by an oximato (N-O) pair; the bridging network is not planar. The more important distortions are observed for the complex having the larger diamino chain. Unexpectedly the latter complex presents an antiferromagnetic interaction, but the related J value is small ($J = -0.49\ cm^{-1}$), whereas in the complex $[CuGd(H_{-2}\mathbf{L27})](NO_3)_3$ the interaction is ferromagnetic ($J = 3.5\ cm^{-1}$) as it is in complexes containing (CuO_2Gd) bridging cores which yield J values varying from 1.4 to $10.1\ cm^{-1}$.

Ward MD synthesized a lot of ligand based on the N,O-bidentate chelating 2-(2-hydroxyphenyl)pyridine unit. The ligand **L29** (6-(2-hydroxyphenyl)pyridine-2-carboxylic acid) having a tridentate phenolate-pyridyl-carboxylate (O,N,O) donor set was found to coordinate transition-metal and lanthanide(III) ions as a dianionic terdentate chelate [30]. Two dinuclear Cu(II) complexes were obtained and crystallographically characterized: $[Cu_2(H_{-2}\mathbf{L29})_2(MeOH)_2]$ has a planar (Cu_2O_2) core with two phenolate ligands bridging the Cu(II) centres, and an axial MeOH ligand on each Cu atom directed to either side of the planar core; in contrast, the axial solvent molecules, one H_2O and one MeOH in $[Cu_2(H_{-2}\mathbf{L29})_2(MeOH)(H_2O)]$, are both on the same face of the (Cu_2O_2) core which induces a substantial 'bowing' of the core to minimize steric interference between them. The ligand **L30** (2-(2-hydroxyphenyl)-4-*t*-butylpyridine) formed the phenolate-bridged dinuclear complex $[Cu_2(H_{-1}\mathbf{L30})_4]$, that is stable in the solid state, but in solution it dissociates to give $[Cu(H_{-1}\mathbf{L30})_2]$ monomeric units [31].

Dinuclear Fe(II)–Fe(III) complexes $[Fe_2(II,III)(H_{-1}\mathbf{L31})(OAc)](OAc)X_2$, where $X = PF_6^-$ or BPh_4^-, were prepared by Maeda using the nonadentate ligand **L31** (4-methyl-2,6-bis[*N*-(2-pyridylmethyl)-*N*-(2-pyridylmethyl-eneaminoethyl)aminomethyl]phenol) (Fig. 12) [32]. Cyclic voltammograms in dried acetonitrile showed a *quasi*-reversible redox couple with $E_1 = -0.07$ V and an irreversible redox couple with $E_2 = 0.58$ V versus SCE for $[Fe_2(II,III)(H_{-1}\mathbf{L31})(OAc)](OAc)(PF_6)_2$, corresponding to a comproportionation constant of 1.0×10^{12}. No visible or near-IR bands due to intervalence electron transitions between Fe(II) and Fe(III) were observed.

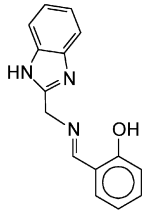

L32

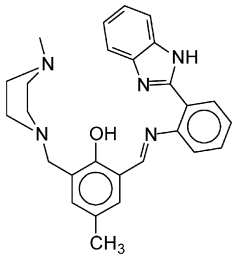

L33

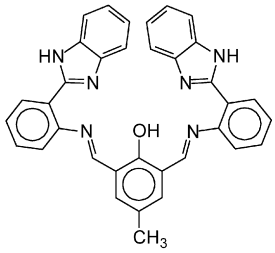

L34

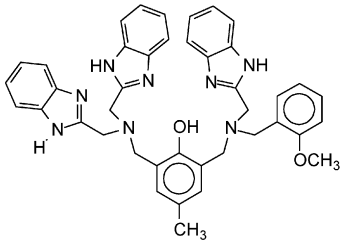

L35

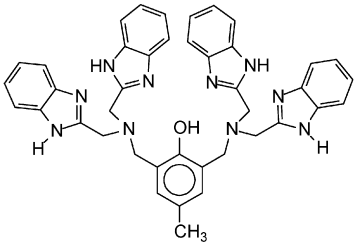

L36

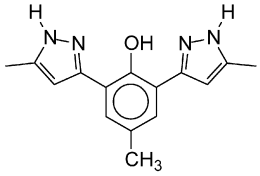

L37

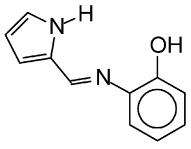

L38

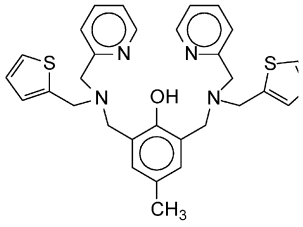

L39

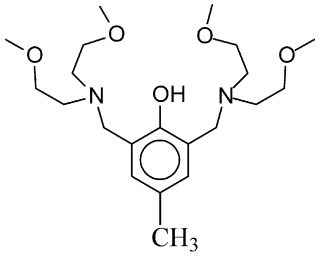

L40

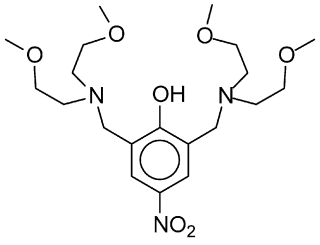

L41

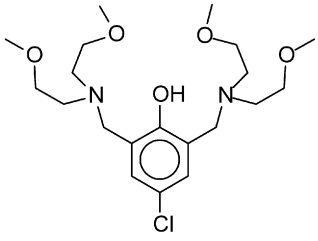

L42

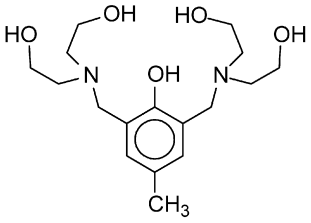

L43

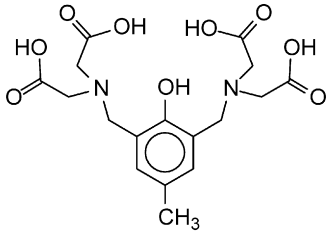

L44

2.1.1.3. Phenolic ligands bearing various heterocycles as side-arms. Reaction between $VO(acac)_2$ and the ONN donor **L32** (2-[(benzimidazol-2-ylmethylimino)methyl]phenol) gave the dinuclear complex $[[V(IV)O(H_{-1}\mathbf{L32})]_2(\mu\text{-}1,3\text{-}SO_4)]$ in which the bridging functions are the phenolate oxygen atoms from both of the ligands and two oxygen atoms of the sulphate group [33].

Kandaswamy co-workers synthesized two dinucleating phenol ligands bearing benzimidazole donors: the symmetrical **L34** (2,6-bis{*N*-[2-(2-benzimidazolyl)-

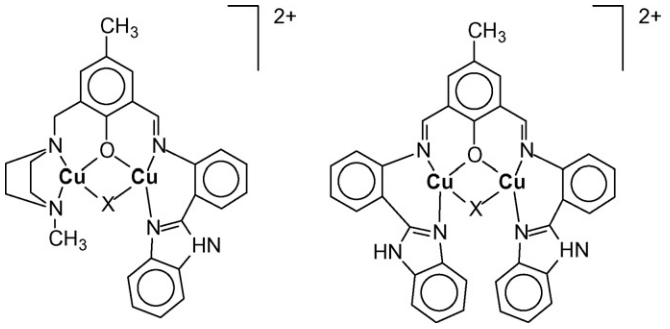

Fig. 13. Proposed structure for the complexes $[Cu_2(H_{-1}\mathbf{L34})(X)]^{2+}$ and $[Cu_2(H_{-1}\mathbf{L33})(X)]^{2+}$.

phenyl]iminomethyl}-4-methylphenol) and the asymmetrical **L33** (2-*N*-[2-(2-benzimidazolyl)phenyl]iminomethyl-6-[(4-methylpiperazin-1-yl)-methyl]-4-methylphenol) [34]. Complexation of these ligands with Cu(II) perchlorate and appropriate sodium salt offered the dinuclear Cu(II) complexes, $[Cu_2(H_{-1}\mathbf{L34})(X)](ClO_4)_2$ and $[Cu_2(H_{-1}\mathbf{L33})(X)](ClO_4)_2$, where X = Cl, OH and OAc (Fig. 13). The authors reported their spectral, electrochemical and magnetic properties. The electrochemical data shows that the complexes of **L33** undergoes reduction at less negatively potential ($E_1 = -0.15$ to -0.25 V, $E_2 = -0.45$ to -0.65 V) when compared to the complexes of **L34** ($E_1 = -0.45$ to -0.58 V, $E_2 = -1.07$ to -1.103 V). A variable temperature magnetic study on the complexes of the ligand **L33** showed strong antiferromagnetic coupling between the copper atoms ($-2J = 285$–$295\ cm^{-1}$), in contrast, the complexes of the ligand **L34** showed weak antiferromagnetic interaction ($-2J = 60$–$85\ cm^{-1}$).

The similar heptadentate ligand **L36** (2,6-bis[bis(2-benzimidazolylmethyl)aminomethyl]-4-methylphenol) was reported by Nie et al. Reaction of $Zn(ClO_4)_2$ with **L36** and sodium isonicotinate yielded a dinuclear Zn complex $[Zn_2(H_{-1}\mathbf{L36})(Iso)(Hiso)](ClO_4)_2$ where Hiso is isonicotinic acid and Iso^- is isonicotinate anion. The structure was established by X-ray crystallography and shows that the two Zn(II) ions are bridged by the phenoxy unit of deprotonated **L36**, and the presence of unusual monodentate O-coordination of the carboxylate group from isonicotinic acid [35]. The coordination geometry around the Zn(II) ion is approximately trigonal bipyramidal. The structure can be regarded as a model for the transition state of the catalytic process of relevant dizinc enzymes.

Rapta and Kamarars reported the synthesis and characterization of a Fe(III) complex featuring a oxo-hydroxo bridge stabilized by hydrogen bonding to uncoordinated benzimidazole moieties of the polydentate asymmetrical ligand **L35** (2-[bis(2-benzimidazolylmethyl)amino]methyl-4-methyl-6-[*N*-(2-benzimidazolylmethyl)-*N*-(2-methoxybenzyl)-aminomethyl]phenol) [36]. This ligand, in ethanolic solution, binds $Fe(ClO_4)_3$ in a 1:1 molar ratio in the presence of hydrogen diphenylphosphate and triethylamine to give $[Fe_2(H\mathbf{L35})_2(\mu\text{-}1,2\text{-}O_2P(OPh)_2)(\mu\text{-}O\cdots H\cdots O)](ClO_4)_4$. Only one branch, the N3, of the ligand coordinates Fe(III), leaving the benzimidazole N–H group and the protonated amine of the N2 branch to

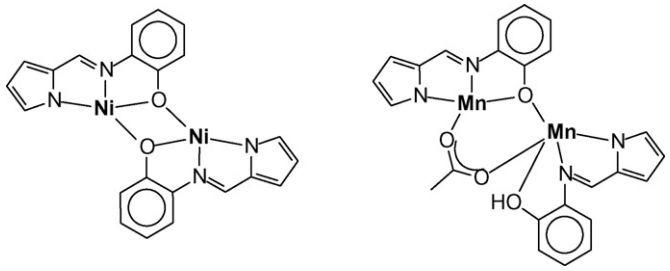

Fig. 14. Proposed structure for the complexes $[Ni_2(H_{-1}\mathbf{L38})_2]$ and $[Mn_2(\mathbf{L38})(H_{-1}\mathbf{L38})(OAc)]$.

hydrogen bond to the oxo-hydroxo and phenoxo moieties, respectively. Coordination at each iron is completed by a N (amine) trans to the oxo-hydroxo bridge, an O (phenolato) trans to the phosphato bridge and two trans-related N (amine) atoms. The authors underlined the importance of the μ-oxo-hydroxo ligand in the catalytic cycle of many enzymes having a diiron core.

The ligand **L37** (4-methyl-2,6-bis(5-methylpyrazol-3-yl)phenol) was able to form phenoxo-bridged homo- and hetero-dinuclear complexes [37]. Variable-temperature magnetic susceptibility measurements carried out for homo-dinuclear $[Cu_2(H_{-1}\mathbf{L37})_2](ClO_4)_2$, $[Cu_2(H_{-1}\mathbf{L37})_2(acac)_2](ClO_4)$, $[Cu_2(H_{-1}\mathbf{L37})(\mu\text{-}OH)Cl_2]$, $[Ni_2(H_{-1}\mathbf{L37})_2(H_2O)_4](ClO_4)_2$ and $[Fe_2(H_{-1}\mathbf{L37})_4(\mu\text{-}OH)_2]$ showed that in all cases the dinuclear metal centres are antiferromagnetically coupled. The ESR spectra of heterodinuclear $[ZnCu(H_{-1}\mathbf{L37})_2](ClO_4)_2$ and $[ZnMn(H_{-1}\mathbf{L37})_2Cl_2]$ were examined. The ^1H NMR spectra of the dicopper(II) complexes $[Cu_2(H_{-1}\mathbf{L37})_2](ClO_4)_2$ and $[Cu_2(H_{-1}\mathbf{L37})_2(acac)_2](ClO_4)$ are reasonably sharp and the isotropic shifts of $[Cu_2(H_{-1}\mathbf{L37})_2](ClO_4)_2$ are relatively smaller compared to those of $[Cu_2(H_{-1}\mathbf{L37})_2(acac)_2](ClO_4)$. The crystal structures of $[Fe_2(H_{-1}\mathbf{L37})_4(\mu\text{-}OH)_2]$ and $[Cu_2(H_{-1}\mathbf{L37})_2(acac)_2](ClO_4)$ were determined. $[Fe_2(H_{-1}\mathbf{L37})_4(\mu\text{-}OH)_2]$ comprises two edge-shared sterically nonequivalent FeO_4N_2 distorted octahedra; the structure of $[Cu_2(H_{-1}\mathbf{L37})_2(acac)_2](ClO_4)$ consists of two nearly square-planar Cu(II) centres supported by a phenoxide bridge.

The ligand **L38** (2-[(2-pyrrolylmethylene)amino]phenol) gives dinuclear complexes $[Cu_2(\mathbf{L35})(H_{-1}\mathbf{L38})(OAc)]$, $[Mn_2(\mathbf{L38})(H_{-1}\mathbf{L38})(OAc)]$, $[Ni_2(H_{-1}\mathbf{L38})_2]$ and $[Co_2(H_{-1}\mathbf{L38})_2]$, synthesized and characterized by Meet's group using IR, UV/vis and MS spectrometry and by elemental analysis [38]. **L38** behaves as a tridentate dianionic ligand in the Co(II) and Ni(II) complexes, while in the Cu(II) and Mn(II) complexes one ligand is a tridentate dianion and the other is a bidentate monoanion (Fig. 14).

The ligand **L39** 4-methyl-2,6-bis{[(2-methylpyridyl)(2-methylthiophenyl)amino]methyl}phenol contains pyridine and thiophene substituents and it yields two dinuclear complexes $[Cu_2(H_{-1}\mathbf{L39})Cl_3]$ and $[Cu_2(H_{-1}\mathbf{L39})Br_3]$ with Cu(II) chloride and bromide. In both complexes, Cu(II) ions are pentacoordinate and bridged by the deprotonated phenolate and by one halogen anion [39]. The complexes were characterized by means of X-ray diffraction, ligand field and EPR spectroscopy, mass spectrome-

try, and electrochemical measurements. Both complexes exhibit geometric asymmetry, as the coordination environment around one of the two copper ions is square-pyramidal, whereas the geometry around the other can be best described as a distorted trigonal bipyramid. The interaction of the complexes with model substrates 3,5-di-*tert*-butylcatecol and tetrachlorocatechol was evaluated by the UV/vis titration of solutions of complexes in acetonitrile with the substrates.

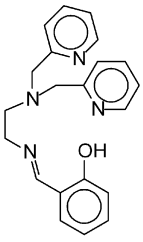

L45

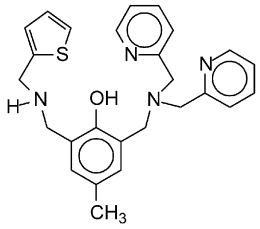

L46

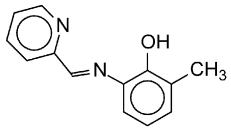

L47

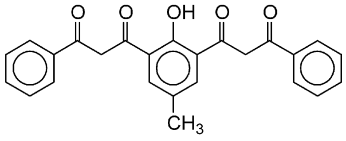

L48

2.1.1.4. Phenolic ligands bearing oxygen donors as side-arms. The ligands **L40** (2,6-bis[bis(2-methoxyethyl)aminomethyl]-4-methylphenol) and his analogues **L41** (2,6-bis[bis(2-methoxyethyl)aminomethyl]-4-nitrophenol), **L42** (2,6-bis[bis(2-methoxyethyl)aminomethyl]-4-chlorophenol) and **L43** (2,6-bis[bis(2-hydroxyethyl)aminomethyl]-4-methylphenol) were extensively investigated by Sakiyama and co-workers [40]. **L40** formed a dinuclear Zn(II) complex $[Zn_2(H_{-1}\mathbf{L40})(OAc)_2]BPh_4$ in which the Zn(II)–Zn(II) separation is 3.264 Å.

X-ray analysis revealed that this complex contains two Zn(II) ions bridged by the phenolic oxygen atom and by two acetate groups, forming a μ-phenoxo-bis(μ-acetato)dizinc(II) core. The dinuclear complex shows an aminopeptidase function which was evaluated using *N*-*p*-nitrophenyl-L-leucine as substrate. Aminopeptidases are enzymes that remove the N-terminal amino acid from a protein or peptide. In order to evaluate the ligand effect on the catalysis, the complexes $[Zn_2(H_{-1}\mathbf{L41})(OAc)_2]BPh_4$ and $[Zn_2(H_{-1}\mathbf{L42})(OAc)_2]BPh_4$ (Fig. 15) were synthesized and studied. The second-order rate constants k for the release of *p*-nitroaniline as the result of the substrate hydrolysis was 2.3×10^{-3} dm^3 mol^{-1} s^{-1} for **L40**, 2.7×10^{-2} dm^3 mol^{-1} s^{-1} for **L41** and 5.9×10^{-1} dm^3 mol^{-1} s^{-1} for **L42**, in the ratio **L42**:**L41**:**L40** = 250:10:1. The aminopeptidase activity was improved 50 times by the substitution of the *p*-methyl group by the *p*-chloro group and 250 times by the substitution of the *p*-methyl group with the *p*-nitro group.

L40 and **L43** give dinuclear species with Co(II) and Ni(II) ions of $[Co_2(H_{-1}\mathbf{L40})(OOCR)_2]BPh_4$, $[Co_2(H_{-1}\mathbf{L43})(OOCR)_2]BPh_4$ and $[Co_2(H_{-1}\mathbf{L40})(OOCR)_2]BPh_4$ stoichiometry, where R = Me or Ph. All these complexes have a μ-phenoxo-bis(μ-carboxylato)dimetallic(II) core and show a ferromagnetic coupling between the two metal ions.

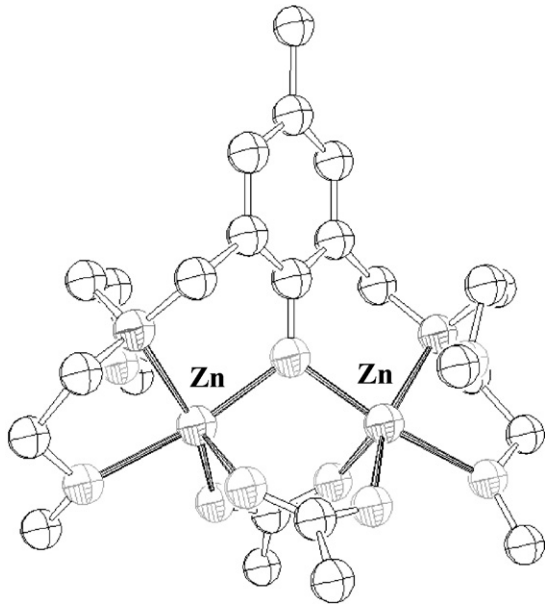

Fig. 15. ORTEP view of the complex cation $[Zn_2(H_{-1}\mathbf{L40})(OAc)_2]^+$.

L44 (2,6-bis[bis(carboxymethyl)aminomethyl]-4-methylphenol) was synthesized as a model for ferritin, the mammalian iron storage protein which consists in a polynuclear iron-oxo core surrounded by a protein shell [41]. A dinuclear complex $[Fe_2(H_{-5}\mathbf{L44})(OH)(H_2O)_2]$ was isolated from acid solution, while a tetranuclear $[Fe_4(H_{-5}\mathbf{L44})_2(O)_2(OH)_2]^4$, having a three-dimensional Fe_4O_6 core, was isolated from basic solution.

2.1.2. Ligand forming dinuclear complexes without μ-phenoxo bridged phenol

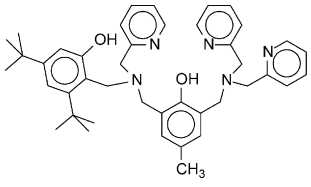

L49

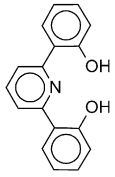

L50

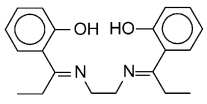

L51

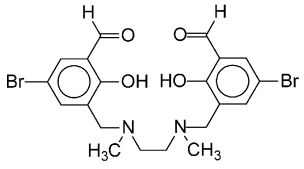

L52

The monophenolic ligand **L45** (*N*,*N*-bis(2-pyridylmethyl)-*N*′-salicylidene-1,2-diaminoethane), forms the dinuclear complex $[Mn(III)_2(O)(H_{-1}\mathbf{L45})_2](ClO_4)_2$ (Fig. 16). The cationic unit $[Mn(III)_2(O)(H_{-1}\mathbf{L45})_2]^{2+}$ contains a linear Mn(III)–O–Mn(III) frame with a Mn-Mn distance of 3.516 Å.

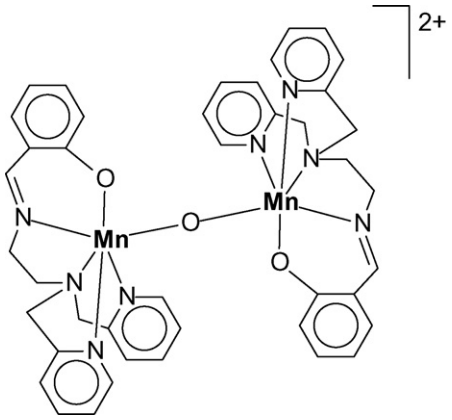

Fig. 16. Structure of the μ-oxo complex $[Mn(III)_2(O)(H_{-1}\mathbf{L45})_2]^{2+}$.

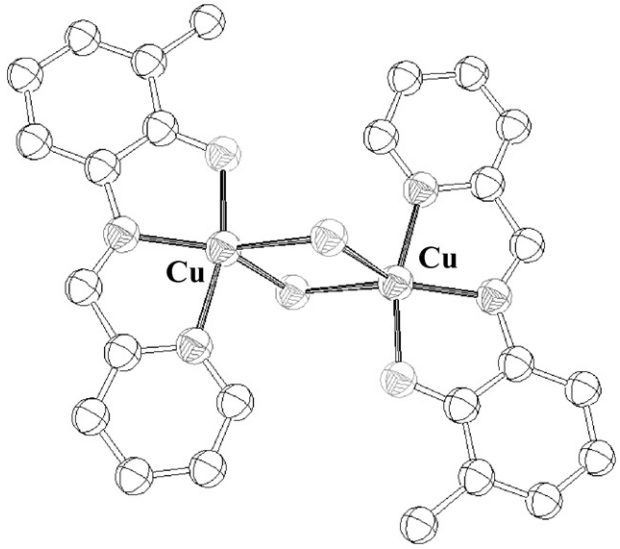

Fig. 17. ORTEP view of the $[Cu(H_{-1}\mathbf{L47})(Cl)]_2$ species.

The pentadentate ligand **L45** wraps around the Mn(III) ion. Electrochemically, it is possible to prepare the one electron oxidized cation $[Mn_2(III,IV)(O)(H_{-1}\mathbf{L45})_2]^{3+}$ which crystallizes as $[Mn_2(III,IV)(O)(H_{-1}\mathbf{L45})_2](ClO_4)_{2.37}(PF_6)_{0.63}$.

The complex cation $[Mn_2(III,IV)(O)(H_{-1}\mathbf{L45})_2]^{3+}$ (Fig. 16) contains a Mn(III)–O-Mn(IV) unit with a Mn-Mn distance of 3.524 Å. The UV/vis spectrum of $[Mn_2(III,IV)(O)(H_{-1}\mathbf{L45})_2]^{3+}$ exhibits an intense absorption band centred at $\lambda = 570$ nm assigned to a phenolate → Mn(IV) charge-transfer transition. The potentials of the redox couples determined by cyclic voltammetry are E° (Mn(III)–Mn(IV)/Mn(III)–Mn(III)) = 0.54 V/SCE and E° (Mn(IV)–Mn(IV)/Mn(III)–Mn(IV)) = 0.99 V/SCE. After oxidation at 1.3 V/SCE, the band at 570 nm shifts to $\lambda = 710$ nm and a well-defined band appears at $\lambda = 400$ nm which suggests the formation of a phenoxyl radical. The relevance of these results to the study of the photosynthetic oxygen evolving complex was discussed [42].

The asymmetrical phenol-based N,O,S-ligand **L46** (2-[(bis(pyridin-2-ylmethyl)amino)methyl]-6-[(thiophen-2-yl)methylamine]-4-methylphenol was used to coordinate Cu(II) chloride [43]. Two dinuclear Cu complexes $[Cu_2(H_{-1}\mathbf{L46})_2(\mu\text{-}Cl)_2](CuCl_4)_2$ and $[Cu_2(H_{-1}\mathbf{L46})_2(\mu\text{-}Cl)_2](ClO_4)_2$ were synthesized and fully characterized. Both the complexes contain a $[Cu_2Cl_2]$ core in which the two Cu(II) ions are bridged by two μ-Cl ligands and have a intermetallic distance of 3.439 Å and 3.525 Å, respectively.

Although the two coordination compounds exhibit identical complex cations, the crystal packings of both molecules significantly differ; they are most likely induced by the distinct tetrachlorocuprate(II) and perchlorate anions.

In order to understand the magnetic interaction between paramagnetic Cu(II) ions in the frame $[Cu_2Cl_2]$, Ma and co-workers synthesized and characterized the μ-Cl bridged dinuclear complex $[Cu(H_{-1}\mathbf{L47})(Cl)]_2$ (Fig. 17) with ligand **L47** (2-methyl-6-[(pyridine-2-ylmethylene)amino]phenol) [44].

The structural study shows the complex has the unusual distorted trigonal-bipyramidal geometry. Variable temperature susceptibility measurements in the range of 2.0–300 K revealed a novel ferromagnetic coupling, $2J = 1.52\ cm^{-1}$. The authors performed a detailed comparison for the magnetic coupling of $[Cu(H_{-1}\mathbf{L47})(Cl)]_2$ with other reported $Cu(\mu\text{-}Cl)_2Cu$ compounds with square-pyramidal or trigonal-bipyramidal geometry. The complex may provide useful information for the magneto-structural correlations of these compounds.

The unusual and interesting ligand **L48** (2,6-bis(1,3-dioxo-3-phenylpropyl)-4-methylphenol) contains two β-diketone units linked to phenol, so as to display an array of five oxygen donors disposed in a linear way [45]. This ligand shows four adjacent coordinating pockets able to chelate an equal number of metal ions in close proximity, in Scheme 3 various complex topologies were reported. Aromì and co-workers reported the behaviour of **L48** towards Cu(II), Mn(II) and Co(II) ions, in presence of several solvents and other co-ligands. All the metal ions tested formed polynuclear complexes, the stoichiometry and structures of them depend by the solvent nature (coordinating or not-coordinating) and by the co-ligands used. The octanuclear clustered polymeric $[Cu_8(H_{-3}\mathbf{L48})_2(OMe)_8X_2]_n$ (X = NO_3, Cl, Br, ClO_4) species were isolated using Cu(II) ions. The cluster can be altered in the tetranuclear analogue $[Cu_4(H_{-3}\mathbf{L48})(OMe)_3X_2]$ by changing the amount of base in solution. This ligand, in non-coordinating solvent, forms with Mn(II) ion the trinuclear trimeric $[Mn_3(H_{-2}\mathbf{L48})_3]$ species in which $H_{-2}\mathbf{L48}^{2-}$ unit exhibits a μ_3 coordination mode with both β-diketonate groups in *syn* conformation with respect to the central phenol group (Scheme 3). Interestingly, if the solvent is coordinating (as pyridine) it participates in the formation of dinuclear complex $[Mn_2(H_{-2}\mathbf{L48})_2(py)_4]$, where the $H_{-2}\mathbf{L48}^{2-}$ unit is μ_2 and it is found in an rare *syn*,*anti* conformation (Scheme 3). The ligand **L48** forms with Co(II) ion di- or trinuclear complexes stable in various conformations; the following series of complexes were synthesized: $[Co_2(H_{-2}\mathbf{L48})_2(solv)_4]$ (solv = py or MeOH), $[Co_2(H_{-2}\mathbf{L48})_2(LL)_2]$ (LL = 2,2′-bipyridine, 2,2′-bipyridylamine, 4,4′-diphenyl-2,2′-bipyridine or 1,10-phenanthroline) and $[Co_3(H_{-2}\mathbf{L48})_3]$. In the $[Co_3(H_{-2}\mathbf{L48})_3]$

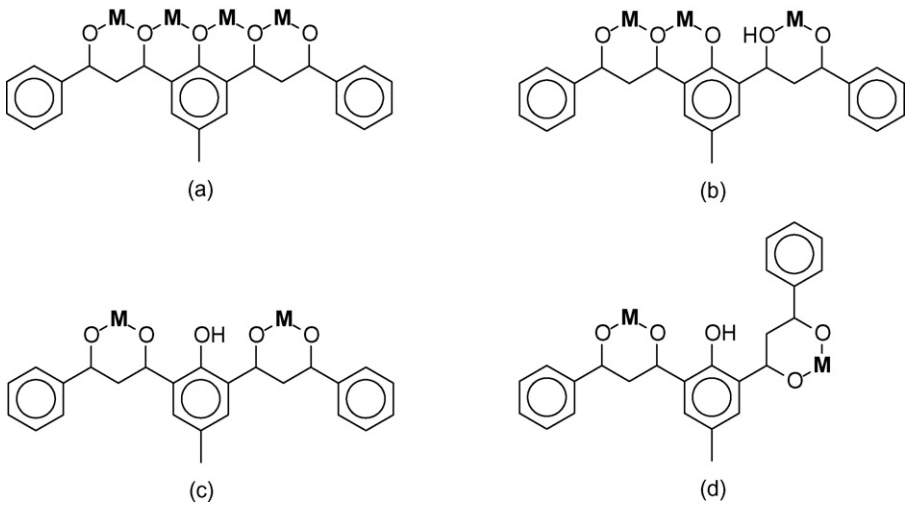

Scheme 3. Representation of all the coordination modes and conformations observed for ligand **L48**: (a) μ_4-*syn*,*syn*; (b) μ_3-*syn*,*syn*; (c) μ_2-*syn*,*syn*; (d) μ_2-*syn*, *anti*.

species the $H_{-2}\mathbf{L48}^{2-}$ unit coordinates three Co(II) ions in μ_3-*syn*,*syn* manner (Scheme 3). In the dinuclear species the $H_{-2}\mathbf{L48}^{2-}$ is μ_2-*syn*,*syn* (e.g $[Co_2(H_{-2}\mathbf{L48})_2(py)_4]$) or μ_2-*syn*,*anti* (e.g $[Co_2(H_{-2}\mathbf{L48})_2(bpy)_2]$), dependently from the co-ligand used.

2.2. Ligands containing two phenolic units

2.2.1. Ligand forming μ-phenoxo dinuclear complexes

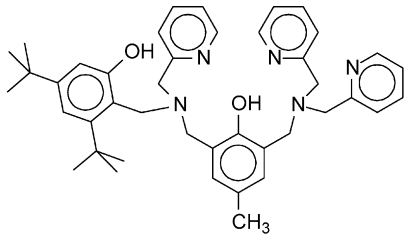

L49

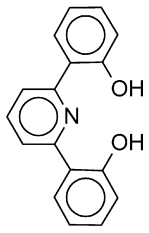

L50

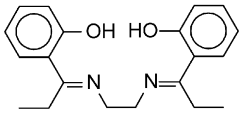

L51

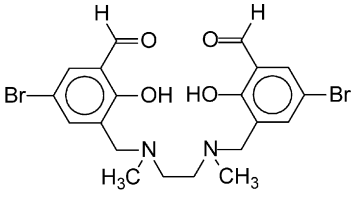

L52

The asymmetrical biphenolic N_5O_2 donor ligand **L49** (2-[*N*,*N*-bis(2-pyridylmethyl)aminomethyl]-6-[*N*′,*N*′-(3,5-di-*tert*-butylbenzyl-2-hydroxy)(2-pyridylmethyl)]-aminomethyl]-4-methylphenol) formed dinuclear Cu(II) complexes $[Cu_2(H_{-1}\mathbf{L49})(\mu\text{-}OCH_3)](ClO_4)_2$ and $[Cu_2(H_{-2}\mathbf{L49})(\mu\text{-}OCH_3)](BPh_4)$; they were synthesized and characterized in the solid state by X-ray crystallography [46]. Both the complexes have a common [Cu(II)(μ-phenoxo)(μ-OCH_3)Cu(II)] structural unit. Magnetic susceptibility studies of $[Cu_2(H_{-1}\mathbf{L49})(\mu\text{-}OCH_3)](ClO_4)_2$ and $[Cu_2(H_{-2}\mathbf{L49})(\mu\text{-}OCH_3)](BPh_4)$ reveal J values of $-38.3\,cm^{-1}$ and $-2.02\,cm^{-1}$, respectively, and that the degree of antiferromagnetic coupling is strongly dependent on the coordination geometries of the Cu centres within the dinuclear [Cu(II)(μ-phenoxo)(μ-OCH_3)Cu(II)] structural unit. Solution studies in CH_2Cl_2, using UV/vis spectroscopy and electrochemistry, indicate that under these experimental conditions the first coordination spheres of the Cu(II) centres are maintained as observed in the solid state structures, and that both forms can be brought into equilibrium $[Cu_2(H_{-1}\mathbf{L49})(\mu\text{-}OCH_3)]^{2+} = [Cu_2(H_{-2}\mathbf{L49})(\mu\text{-}OCH_3)]^{+} + H^{+}$ by adjusting the pH. Potentiometric titration studies of $[Cu_2(H_{-1}\mathbf{L49})(\mu\text{-}OCH_3)](ClO_4)_2$ in an EtOH/H_2O mixture (70:30, v/v; $I = 0.1\,mol\,dm^{-3}$ KCl) show three titratable protons, indicating the dissociation of the bridging CH_3O– group (Scheme 4).

The catecholase activity of $[Cu_2(H_{-1}\mathbf{L49})(\mu\text{-}OCH_3)](ClO_4)_2$ and $[Cu_2(H_{-2}\mathbf{L49})(\mu\text{-}OCH_3)](BPh_4)$ in MeOH/H_2O buffer (30:1, v/v) demonstrates that the deprotonated form is the active species in the oxidation of 3,5-di-*tert*-butylcatechol and that the reaction follows Michaelis–Menten behaviour with $k_{cat} = 5.33 \times 10^{-3}\,s^{-1}$ and $K_M = 3.96 \times 10^{-3}\,mol\,dm^{-3}$. The complex $[Cu_2(H_{-2}\mathbf{L49})(\mu\text{-}OCH_3)](BPh_4)$ can be electrochemically oxidized with $E_{1/2} = 0.27\,V$ versus ferrocenium/ferrocene couple Fc^+/Fc, a redox potential which is believed to be related to the formation of a phenoxyl radical. Since these complexes are redox active species, the authors analyzed their activity towards the nucleic acid DNA, a macromolecule prone to oxidative damage. These complexes promoted DNA cleavage following an oxygen-dependent pathway.

Wang synthesized dinuclear and tetranuclear Cu(II) complexes, based on the ligand **L50** (2,6-bis(2-hydroxyphenyl) pyridine), of stoichiometry $[Cu_2(H_{-2}\mathbf{L50})_2(Py)_2]$ and

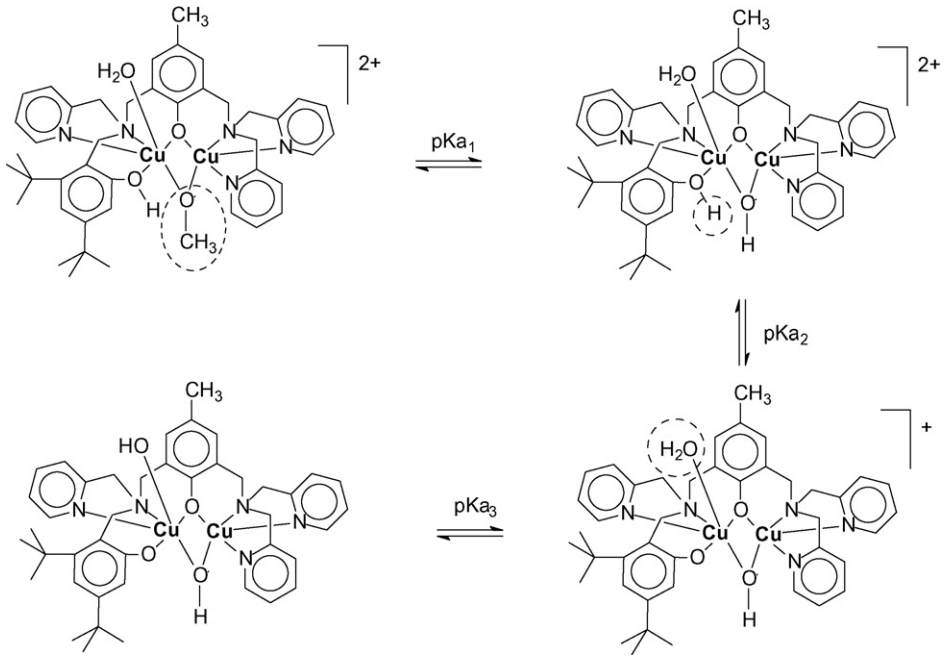

pK_{a1}	5.23
pK_{a2}	5.94
pK_{a3}	7.59

Scheme 4. pK_a values of complex $[Cu_2(H_{-1}\mathbf{L49})(\mu\text{-OCH3})]^{2+}$ determined by potentiometric titration at 298.1 K in an EtOH/H_2O mixture (70:30, v/v; $I = 0.1$ mol dm^{-3} KCl).

$[Cu_4(H_{-2}\mathbf{L50})_4(DMF)]$. These complexes were characterized by elemental analyses, mass spectrometry, and single-crystal X-ray diffraction analyses [47]. $[Cu_2(H_{-2}\mathbf{L50})_2(Py)_2]$ is a dinuclear complex with two Cu(II) centres, two pyridine ligands, and two $H_{-2}\mathbf{L50}$ ligands; each $H_{-2}\mathbf{L50}$ ligand donates its pyridyl ring and one of the phenolate groups to one metal and shares the other phenolate group between both metals, affording a $Cu_2(\mu\text{-O})_2$ core. On the contrary, $[Cu_4(H_{-2}\mathbf{L50})_4(DMF)]$ is a tetranuclear complex with four Cu(II) centres and four $H_{-2}\mathbf{L50}$ ligands. Two of the $H_{-2}\mathbf{L50}$ ligands have the same coordination mode as $[Cu_2(H_{-2}\mathbf{L50})_2(Py)_2]$, while the other two $H_{-2}\mathbf{L50}$ ligands donate their pyridyl rings to one metal and share both phenolate groups between four metals, resulting in three four-membered $Cu_2(\mu\text{-O})_2$ rings, which joined each other and showed great distortion from planarity. The ligand forms also a Zn(II) tetranuclear complex with four Zn(II) centres, four pyridine and four $H_{-2}\mathbf{L50}$ ligands; the $H_{-2}\mathbf{L50}$ ligands have the same coordination modes as those of $[Cu_4(H_{-2}\mathbf{L50})_4(DMF)]$.

Heterodinuclear Cu(II)–Gd(III) and Ni(II)–Gd(III) complexes were obtained from the open diphenolic ligands **L51** (3,8-bis(2-hydroxyphenyl)-4,7-diazadeca-3,7-diene) and **L52** (*N*,*N*′-dimethyl-*N*,*N*′-bis[(5-bromo-3-formyl-2-hydroxyphenyl)methyl]ethylendiamine) (Fig. 18). **L51** formed two dinuclear complexes [48] $[CuGd(H_{-2}\mathbf{L51})(hfa)_3]$, $[NiGd(H_{-2}\mathbf{L51})(hfa)_3]$. Both $[CuGd(H_{-2}\mathbf{L51})(hfa)_3]$ and $[NiGd(H_{-2}\mathbf{L51})(hfa)_3]$ are discrete dinuclear complexes consisting of an eight coordinate Gd(III) ion which is bridged to four coordinate Cu(II) or Ni(II) ion via both phenolate oxygen atoms of the ligand **L51**. The crystal structure shows no tendency towards dimerization between adjacent Cu(II) Schiff base units in $[CuGd(H_{-2}\mathbf{L51})(hfa)_3]$. Cryomagnetic measurements, as predicted by theory, show a ferromagnetic interaction between Gd(III) and Cu(II) in $[CuGd(H_{-2}\mathbf{L51})(hfa)_3]$ with $J = 1.91$ cm^{-1}. **L52** formed a Cu(II)–Gd(III) heterodinuclear complex $[CuGd(H_{-2}\mathbf{L52})(OAc)(H_2O)](ClO_4)$ that dimerized to form a tetranuclear $[CuGd]_2$ complex

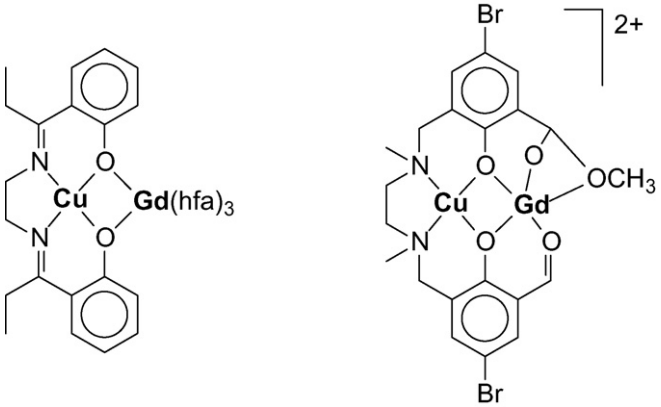

Fig. 18. Structure of the complexes $[CuGd(H_{-2}\mathbf{L51})(hfa)_3]$ and $[CuGd(H_{-3}\mathbf{L52}_{hemiacetal})]^{2+}$.

$[CuGd(H_{-2}\mathbf{L52})(OAc)(H_2O)]_2(ClO_4)_2$. Structural analysis of $[CuGd(H_{-2}\mathbf{L52})(OAc)(H_2O)]_2(ClO_4)_2$ revealed that one of the two formyl groups of the ligand is converted into a hemiacetal group and the two dinuclear Cu(II)–Gd(III) units are bridged by the alcoholic oxygen atoms of acetal groups of each unit to built the tetranuclear $[CuGd]_2$ core.

2.2.2. Ligand forming dinuclear complexes without μ-phenoxo bridged phenol

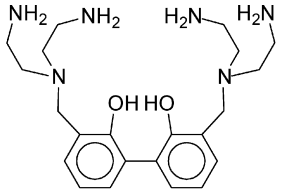

L53

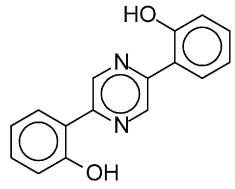

L54

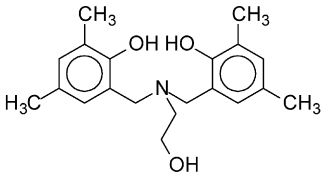

L55

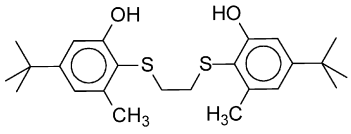

L56

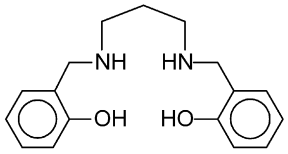

L57

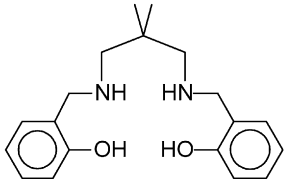

L58

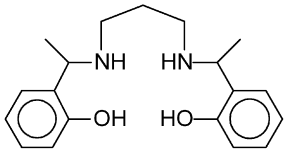

L59

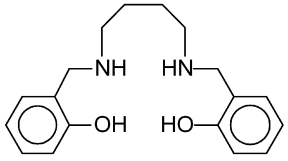

L60

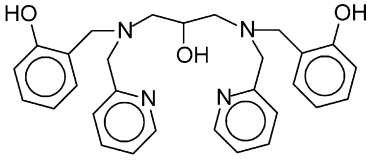

L61

The biphenolic ligand **L53** (3,3′-bis[*N*,*N*-bis(2-aminoethyl)aminomethyl]-2,2′-dihydroxybiphenyl) contains two diethylenetriamine units linked by a 1,1′-bis(2-phenol) group on the central nitrogen atom which allows two separate binding amino subunits in a non-cyclic ligand [49].

The basicity and binding properties of **L53** towards Cu(II) and Zn(II) ions were determined by means of potentiometric measurement in aqueous solution (298.1 K, $I = 0.15$ mol dm^{-3}). **L53** behaves as a pentaprotic base and as a monoprotic acid under the experimental conditions used, yielding the $H_5\mathbf{L53}^{5+}$ or $H_{-1}\mathbf{L53}^{-}$ species, respectively (Table 10).

L53 formed both mononuclear and dinuclear species with both metal ions investigated; the dinuclear species are largely prevalent in aqueous solution with a **L53**/M(II) molar ratio of 1:2 at pH higher than 7.

L53 shows different behaviour in Cu(II) and Zn(II) binding (Table 11), affecting the dinuclear species formed and the distance between the two coordinated metal ions, which is greater in the Zn(II) than in the Cu(II) dinuclear species. This difference can be attributed to the different degree of protonation of biphenol moiety which influence the angle between the phenyl rings in the two systems. In this way, it was possible to modulate the M(II)–M(II) distance by the choice of M(II) and to space the two M(II) farther away than was possible with the previously synthesized analogous ligands **L1** and

Table 10
Protonation constants (log *K*) of **L53** determined by means of potentiometric measurements in 0.15 mol dm^{-3} NaCl aqueous solution at 298.1 K

Reaction	log *K*
$H_{-1}\mathbf{L53}^{-} + H^+ = \mathbf{L53}$	10.58(4)[a]
$\mathbf{L53} + H^+ = H\mathbf{L53}^{+}$	10.52(1)
$H\mathbf{L53}^{+} + H^+ = H_2\mathbf{L53}^{2+}$	9.56(1)
$H_2\mathbf{L53}^{2+} + H^+ = H_3\mathbf{L53}^{3+}$	9.34(1)
$H_3\mathbf{L53}^{3+} + H^+ = H_4\mathbf{L53}^{4+}$	6.09(2)
$H_4\mathbf{L53}^{4+} + H^+ = H_5\mathbf{L53}^{5+}$	3.78(4)

[a] Values in parentheses are the standard deviations on the last significant figure.

Table 11
Logarithm of the equilibrium constants determined in 0.15 mol dm^{-3} NaCl at 298.1 K for the complexation reactions of **L53** with Cu(II) and Zn(II) ions

Reaction	log *K*	
	Cu(II)	Zn(II)
$M^{2+} + H_{-1}\mathbf{L53}^{-} = M(H_{-1}\mathbf{L53})^{+}$	20.52(3)[a]	14.79(3)
$M + \mathbf{L53} = M\mathbf{L53}^{2+}$	19.61(2)	13.85(3)
$M(H_{-1}\mathbf{L53})^{+} + H^+ = M\mathbf{L53}^{2+}$	9.67(2)	9.64(3)
$M\mathbf{L53}^{2+} + H^+ = M(H\mathbf{L53})^{3+}$	7.83(2)	8.87(2)
$M(H\mathbf{L53})^{3+} + H^+ = M(H_2\mathbf{L53})^{4+}$	4.81(1)	5.05(2)
$M(H_{-1}\mathbf{L53})^{+} + H^+ = M_2(H_{-1}\mathbf{L53})OH$	2.58(3)	
$M_2(H_{-1}\mathbf{L53})^{3+} + OH^- = M_2H_{-1}\mathbf{L53}^{4+}$	4.07(3)	
$M^{2+} + M(H_{-1}\mathbf{L53})^{+} = M_2(H_{-1}\mathbf{L53})^{3+}$	13.77(2)	8.84(2)
$M_2(H_{-1}\mathbf{L53})^{3+} + OH^- = M_2(H_{-1}\mathbf{L53})OH^{2+}$	8.44(3)	
$M_2(H_{-1}\mathbf{L53})OH^{2+} + OH^- = M_2(H_{-1}\mathbf{L53})(OH)_2{}^{+}$	2.31(4)	
$M_2(H_{-1}\mathbf{L53})^{3+} = M_2(H_{-2}\mathbf{L53})^{2+} + H^+$		−6.72(2)
$M_2(H_{-2}\mathbf{L53})^{2+} + OH^- = M_2(H_{-2}\mathbf{L53})OH^{+}$		3.98(3)
$M_2(H_{-2}\mathbf{L53})OH + OH^- = M_2(H_{-2}\mathbf{L53})(OH)_2{}^{+}$		3.06(3)

[a] Values in parentheses are the standard deviations on the last significant figure.

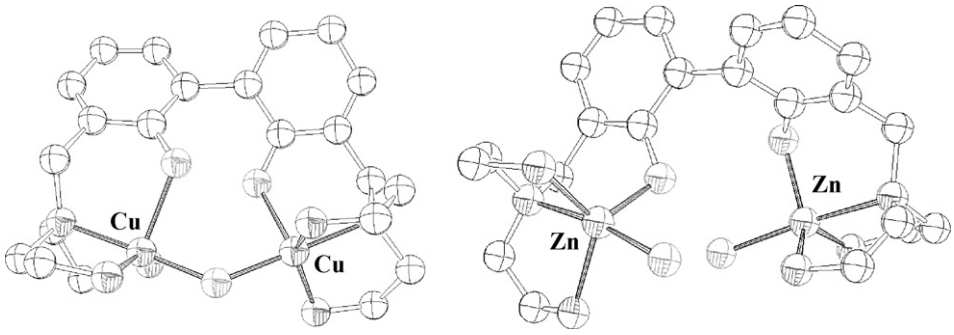

Fig. 19. ORTEP view of the complex cations $[Cu_2(H_{-1}\mathbf{L53})(OH)]^{2+}$ and $[Zn_2(H_{-2}\mathbf{L53})(H_2O)_2]^{2+}$.

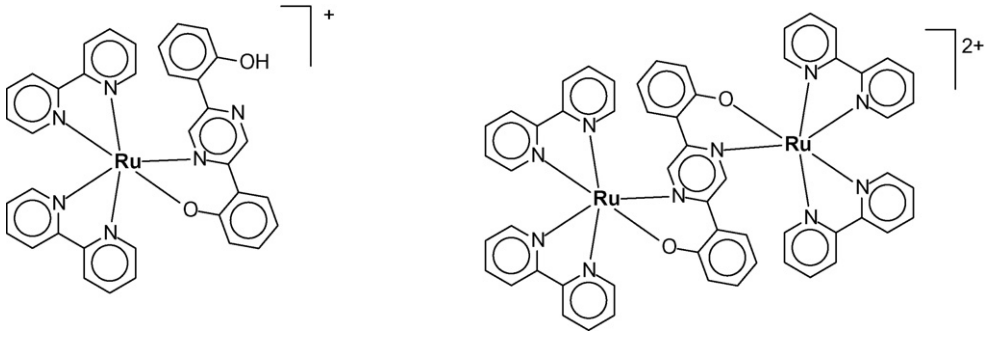

Fig. 20. Structure for the cationic mononuclear and dinuclear complexes $[Ru(bpy)_2(H_{-1}\mathbf{L54})]^{+}$ and $[Ru(bpy)_2(H_{-2}\mathbf{L54})Ru(bpy)_2]^{2+}$.

L2. **L53** formed the complex cations $[Zn_2(H_{-2}\mathbf{L53})(H_2O)_2]^{2+}$ (Zn(II)–Zn(II) distance = 4.962 Å) and $[Cu_2(H_{-1}\mathbf{L53})(OH)]^{2+}$ (Cu(II)–Cu(II) distance = 3.546 Å) in which the coordination sphere of the metal ions are not saturated, and thus, these latter species are prone to add guests (Fig. 19). Both the complexes were characterized by X-ray and UV/vis spectroscopy, and the complex $[Zn_2(H_{-2}\mathbf{L53})(H_2O)_2]^{2+}$ by ^{1}H NMR and ^{13}C NMR experiments.

The ligand **L54** (3,5-bis(2-hydroxyphenyl)pyrazine) was able to form dinuclear Ru(II) complexes $[Ru(bpy)_2(H_{-2}\mathbf{L54})Ru(bpy)_2](PF_6)_2$, in which each Ru(II) moieties are bound throughout adjacent O,N coordination to anionic phenolate and a pyrazine bridge (Fig. 20) [50]. Relatively few reports are available on the dinuclear complexes bridged across a phenolate and this study provides an opportunity to examine the impact of reduced O donor ligands on metal–metal communication. The authors presented very unusual behaviour whereby the apparent location of the LUMO changes between the mononuclear $[Ru(bpy)_2(H_{-1}\mathbf{L54})](PF_6)$ and dinuclear $[Ru(bpy)_2(H_{-2}\mathbf{L54})Ru(bpy)_2](PF_6)_2$ complexes. The lowest energy optical transition appears to involve the peripheral bipyridine ligand as acceptor in the mononuclear complex, whereas this ligand is not involved in the lowest energy optical transition in the dinuclear complex.

The origin of this difference is not clear, however, significant changes in the electronic properties of the mononuclear complex are observed on coordination of the second metal, reflected in significant alterations in the electrochemistry of the bridge and metals as well as changes in the optical spectroscopy.

In order to extract in organic solvents the uranyl(VI) cation, UO_2^{2+}, a series of biphenolic ligand bearing an alcoholic chain and a tertiary aminic function was examined [51]. Among them, **L55** (*N*,*N*-bis(2-hydroxy-3,5-dimethylbenzyl)-2-aminoethanol), reacts with uranyl nitrate hexahydrate and in acetonitrile without base, affording the dinuclear uranyl complex $[(UO_2)_2(H_{-1}\mathbf{L55})_2(NO_3)_2]$. The molecular structures of this complex were verified by X-ray crystallography whereby it was ascertained that it is a dialkoxo-bridged dinuclear uranyl complex with a U(VI) to **L55** ratio of 1:1.

In order to better understanding the molecular mechanism and the origin of stereoselectivity in the polymerization of styrene, Okuda and co-workers designed and realized a series of new group IV metal catalysts bearing 1,ω-dithiaalcanediyl-bridged bis-phenolate ligands [52]. In particular, ligand **L56** (1,4-dithiabutanediyl-2,2′-bis(6-*tert*-butyl-4-methylphenol) was reacted with $[Ti(OiPr)_2((R)\text{-binol})]$ affording the chiral-at-metal complex $[Ti(H_{-2}\mathbf{L56})((R)\text{-binol})]$ in low diastereomeric excess. Complex $[Ti(H_{-2}\mathbf{L56})((R)\text{-binol})]$, after partial hydrolysis, gave dinuclear complex $[Ti_2(H_{-2}\mathbf{L56})_2(\mu\text{-}(R)\text{-binol})(\mu\text{-O})]$, in which the two Ti(IV) centres are homochiral and are bridged by the ((*R*)-binol) unit and by a (μ-O) ligand (Fig. 21). The molecular structure of $[Ti(H_{-2}\mathbf{L56})((R)\text{-binol})]$ and $[Ti_2(H_{-2}\mathbf{L56})_2(\mu\text{-}(R)\text{-binol})(\mu\text{-O})]$ was confirmed by single crystal X-ray analysis, which shows C_2-symmetry in both complexes.

Dinuclear complexes bearing O = Re(V)–O–Re(V) = O and O = Tc(V)–O–TC(V) = O frames are extensively studied due the applications of radioactive isotopes ^{186}Re, ^{188}Re and ^{99m}Tc in radiopharmaceutical for radiotherapy.

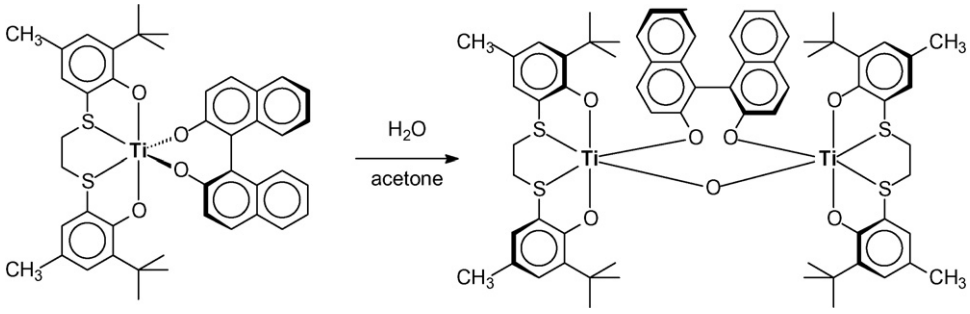

Fig. 21. Structure of the mononuclear and dinuclear complexes [Ti(H$_{-2}$**L56**)((*R*)-binol)] and [Ti$_2$(H$_{-2}$**L56**)$_2$(μ-(*R*)-binol)(μ-O)].

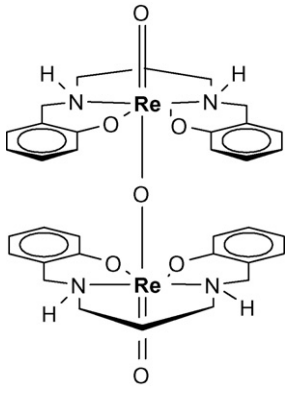

Fig. 22. Structure of the complex [Re$_2$(H$_{-2}$**L57**)$_2$(O)$_2$(μ-O)] bearing the O=Re–O–Re=O backbone.

In order to achieve better stabilization of these moieties, Sclemper's group synthesized tetradentate amino diphenolic ligands **L57** (*N*,*N*′-bis[(2-hydroxyphenyl]methyl)-1,3-propylendiamine), **L58** (*N*,*N*′-bis[(2-hydroxyphenyl]methyl)-2,2-dimethyl-1,3-propylendiamine), **L59** (*N*,*N*′-bis[1-(2-hydroxyphenyl)ethyl]-1,3-propylendiamine), **L60** (*N*,*N*′-bis[(2-hydroxyphenyl]methyl)-1,4-butylendiamine) [53]. The ligand **L57**, **L58** and **L60** formed dinuclear Tc(V) complexes [Tc$_2$(H$_{-2}$**L57**)$_2$(O)$_2$(μ-O)] (Fig. 22), [Tc$_2$(H$_{-2}$**L58**)$_2$(O)$_2$(μ-O)] and [Tc$_2$(H$_{-2}$**L60**)$_2$(O)$_2$(μ-O)] containing the O=Tc–O–Tc=O backbone. The ligand **L57**, **L59** and **L60** formed dinuclear Re(V) complexes [Re$_2$(H$_{-2}$**L57**)$_2$(O)$_2$(μ-O)], [Re$_2$(H$_{-2}$**L59**)$_2$(O)$_2$(μ-O)] and [Re$_2$(H$_{-2}$**L60**)$_2$(O)$_2$(μ-O)] containing the O=Re–O–Re=O backbone. All the complexes were characterized by ^{1}H NMR, ^{13}C NMR, IR spectroscopy, UV/vis spectroscopy and X-ray diffraction analysis. The complexes shows a near octahedral M(V) coordination.

Fenton and co-workers, in order to realize biomimetic dinuclear Zn(II) complexes as model of hydrolase, synthesized a series of polypodal ligands based on pyridine moiety [54]. Among these new molecules, the authors reported the ligand **L61** (1,3-bis(2-xydroxybenzylpyridn-2-ylmethylamino)propan-2-olo) and its dinuclear Zn(II) complex [Zn$_2$(H$_{-3}$**L61**)(OAc)]. In this complex the two Zn(II) ions are bridged by the deprotonated alcoholic oxygen atom of the ligand H$_{-3}$**L61**$^{3-}$ and by a μ-1,3-acetate anion (Fig. 23).

2.3. Ligands containing three or more phenolic units

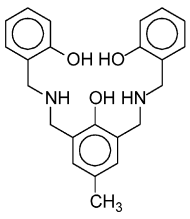

L62

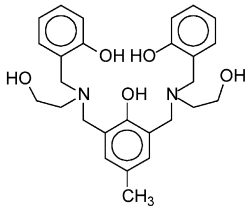

L63

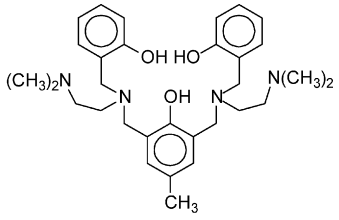

L64

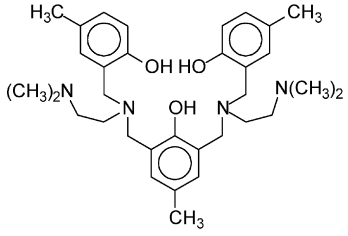

L65

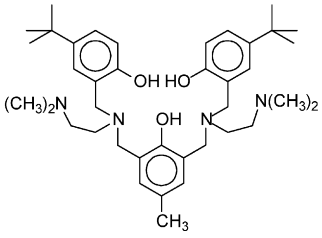

L66

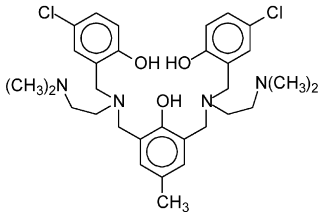

L67

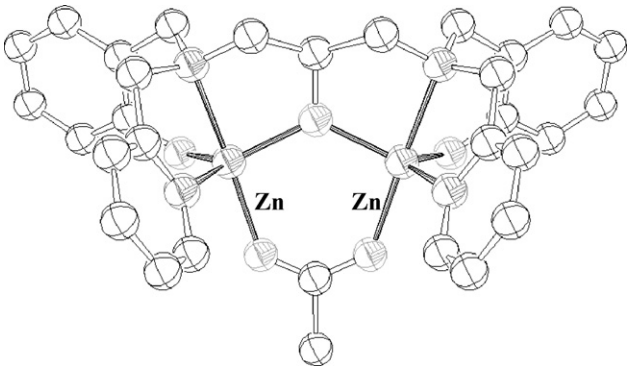

Fig. 23. ORTEP view of the $[Zn_2(H_{-3}\mathbf{L61})(OAc)]$ species.

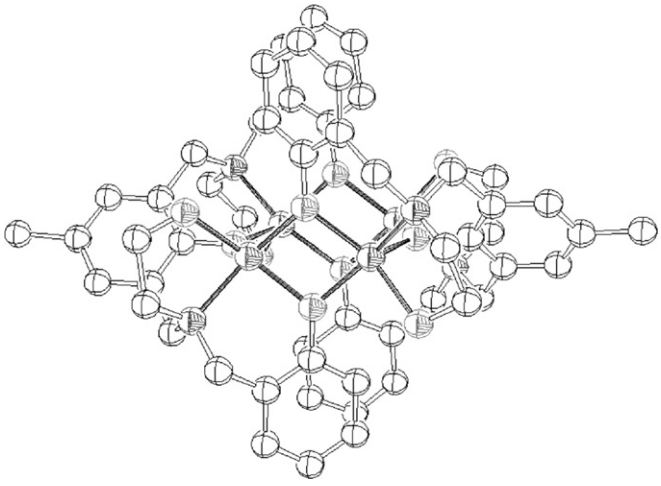

Fig. 24. ORTEP view of the complex cation $[Zn_4(H_{-3}\mathbf{L63})_2]^{2+}$.

A series of amino-triphenolic ligands bearing the pentadentate N_2O_3 donor bis(aminomethyl)triphenol moiety were synthesized by many research groups. Here we report the coordination properties of more representative ligands of this class towards transition metal ions.

Nag and co-workers synthesized and characterized the ligand **L62** (2,6-bis{[(2-hydroxyphenyl)methyl]aminomethyl}-4-methylphenol), that formed the stable dinuclear dimeric Fe(III) complex $[Fe_2(H_{-3}\mathbf{L62})_2]$. In this complex the two Fe(III) ions are bridged by the central cresolate group of each ligand, forming a $[Fe_2O_2]$ core[37]. Each Fe(III) ions is hexacoordinated by two nitrogen atoms of the amine function and by two oxygen atoms of the terminal phenolate ions of one ligand, and by two oxygen atoms of the central cresolate moieties of both ligands, thus to have a N_2O_4 coordination sphere.

The ligand **L63** ((2,6-bis{*N*-[(2-hydroxyphenyl)methyl]-*N*-(2-hydroxyethyl)aminomethyl}-4-methylphenol) is analogue to **L62** with two 2-hydroxyethyl frames linked to the two nitrogen atoms [55]. **L63** is a potentially heptadentate N_2O_5 ligand forming the tetranuclear Zn(II) complex $[Zn_4(H_{-3}\mathbf{L63})_2](ClO_4)_2$ (Fig. 24). The three-dimensional $[Zn_4O_6]$ core of this species is formed by four Zn(II) ions bridged by two cresolic and four phenolic oxygen atoms of two ligands. All four Zn(II) centres are pentacoordinated and adopt a distorted square pyramid geometry. The complex is stable and strongly fluorescent at $\lambda_{em} = 330$ nm ($\lambda_{ex} = 298$ nm), which were quenched by the presence of dihydrogen phosphate anion in methanol.

Thus $[Zn_4(H_{-3}\mathbf{L63})_2](ClO_4)_2$ can be used as selective sensor for dihydrogen phosphate anion. The binding phenomenon was monitored by UV/vis absorption, fluorescence quenching effects, ESI-MS techniques and NMR studies. The

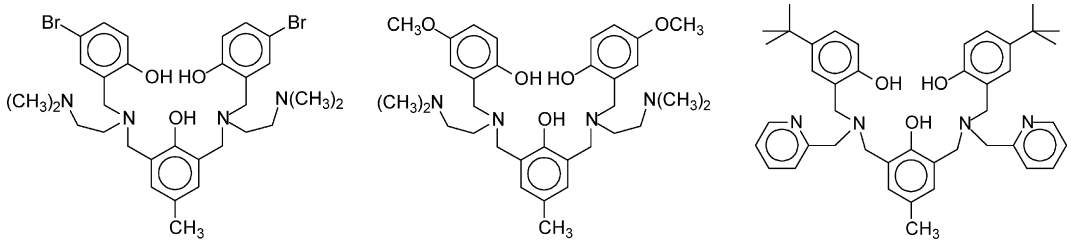

L68 **L69** **L70**

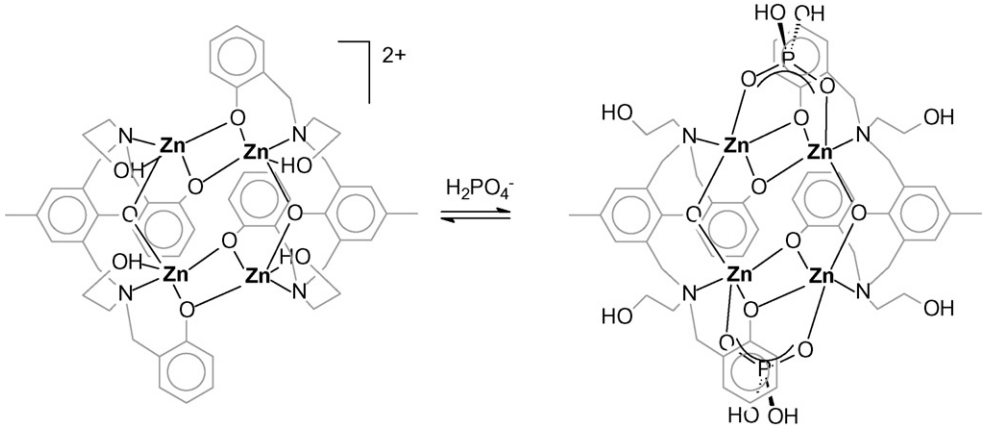

Fig. 25. Proposed 2:1 binding mode of $H_2PO_4^-$ to the tetranuclear $[Zn_4(H_{-3}\mathbf{L63})_2]^{2+}$ complex.

potential binding mode is represented in Fig. 25; the adduct $[Zn_4(H_{-3}\mathbf{L63})_2(H_2PO_4)]$ shows each dihydrogen phosphate anion bridging in a μ-1,3 mode two Zn(II) ions and taking place of the two alcoholic ligands.

The N_4O_3 coordinating ligands **L64** (2,6-bis[{{(2-hydroxybenzyl)(*N*′,*N*′-(dimethylamino)ethyl)}amino}methyl]-4-methylphenol, **L65** (2,6-bis[{{(5-methyl-2-hydroxybenzyl)(*N*′,*N*′-(dimethylamino)ethyl)}amino}methyl]-4-methylphenol), **L66** (2,6-bis[{{(5-*tert*-butyl-2-hydroxybenzyl)(*N*′,*N*′-(dimethylamino)ethyl)}amino}methyl]-4-methylphenol), **L67** (2,6-bis[{{(5-chloro-2-hydroxybenzyl)(*N*′,*N*′-(dimethylamino)ethyl)}amino}methyl]-4-methylphenol), **L68** (2,6-bis[{{(5-bromo-2-hydroxybenzyl)(*N*′,*N*′-(dimethylamino)ethyl)}amino}-methyl]-4-methylphenol), and **L69** (2,6-bis[{{(5-methoxy-2-hydroxybenzyl)(*N*′,*N*′-(dimethylamino)ethyl)}methyl}]-4-methylphenol), were used to synthesize dinuclear V(IV)–V(V) oxophenoxovanadates [56].

The chemistry of mixed-valence vanadium complexes is of abiding interest because they play an important role in different biological processes and offers easy success to the model system $[3d^1,3d^0]$ to understand the behaviour of the unpaired electron and hence the oxidation state of metal both in solid state and in solution. The ligands **L64–L69** were designed and synthesized to realize dinuclear V(IV)–V(V) complexes having $[V_2(H_{-3}\mathbf{L})(\mu\text{-}O)(O)_2]$ general stoichiometry (**L** = **L64**, **L65**, **L66**, **L67**, **L68** and **L69**). For example, in $[V_2(H_{-3}\mathbf{L64})(\mu\text{-}O)(O)_2]$, both the metal atoms have distorted octahedral geometry, with a V(IV)–V(V) distance of 3.173 Å (Fig. 26). The two metal ions are bridged by the oxygen atom of the central cresolate anion of $H_{-3}\mathbf{L64}$ and by a (μ-O) ligand, forming a symmetrical $[O{=}V(\mu\text{-}O_{oxo})(\mu\text{-}O_{cresolate})V{=}O]$ core. X-ray crystallography, IR, UV–visible, and ^{1}H NMR and ^{51}V NMR experiments (complexes are NMR-silent) show that the mixed-valence complexes contain two indistinguishable V atoms.

The new ligand **L70** (2,6-bis{[(2-hydroxy-5-*tert*-butylbenzyl)(2-pyridylmethyl)amino]methyl}-4-methylphenol), which contains two additional phenolate groups and two *tert*-butyl groups compared to its parent monophenolic **L21**, is able to stabilize two Mn(III) ions forming the high valent complex [57] $[Mn(III)_2(H_{-3}\mathbf{L70})(\mu\text{-}OAc)_2](PF_6)$. High valent polynuclear Mn complexes have a crucial role in artificial photosynthesis processes, which are a target in the search for continuable energy resources. Previously, reporting the properties of ligand **L21**, we highlighted that this ligand is not able to forms Mn(III)–Mn(III) dinuclear complexes, but it stabilizes Mn(III)–Mn(II) complexes. The stronger bond between oxygen of lateral phenolate groups of **L70** and Mn than that between neutral nitrogen of pyridine of **L21** and Mn, prevents the dissociation of central ions. The new complex $[Mn(III)_2(H_{-3}\mathbf{L70})(\mu\text{-}OAc)_2](PF_6)$ and $[Mn_4]$ cluster present in natural oxygen evolving centres (OEC in nature) are very similar. In the complex $[Mn_2(H_{-3}\mathbf{L70})(\mu\text{-}OAc)_2](PF_6)$ the two Mn(III) ions are bridged by a μ-phenoxo moiety and by two acetate anions, in a μ-1,3 mode.

3. Macrocyclic ligands

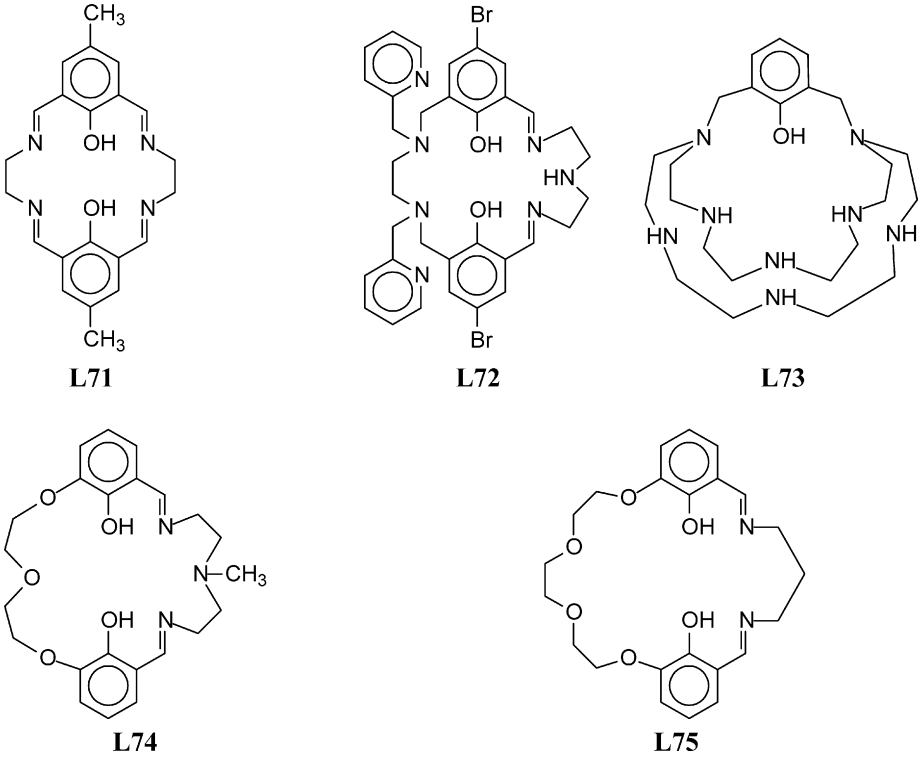

L71 **L72** **L73**

L74 **L75**

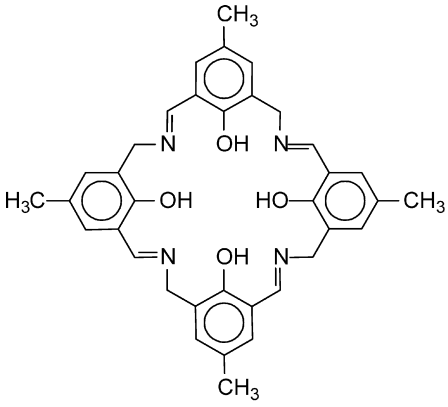

L76

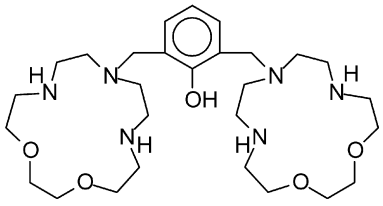

L77

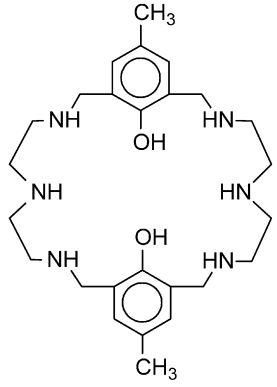

L78

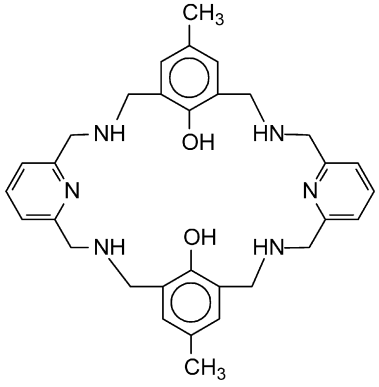

L79

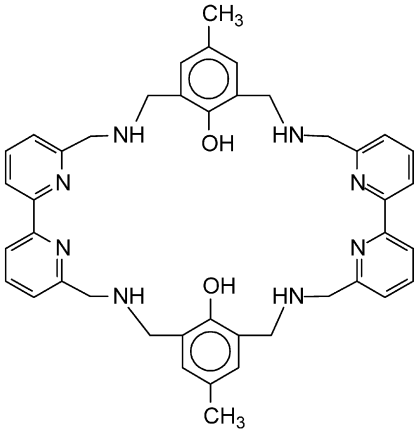

L80

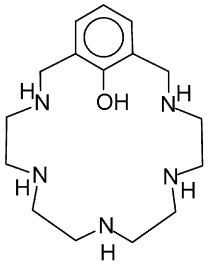

L81

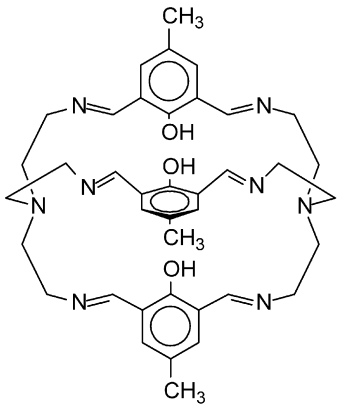

L82

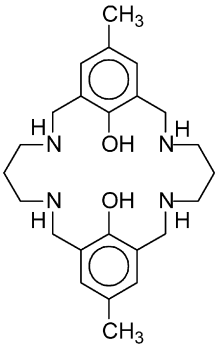

L83

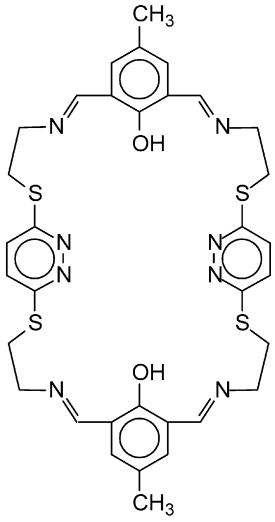

L84

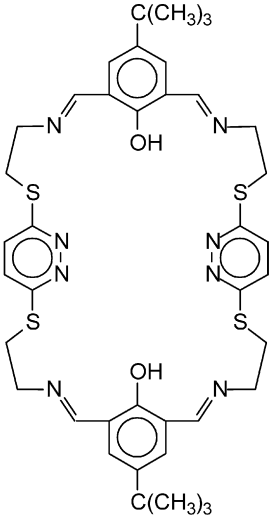

L85

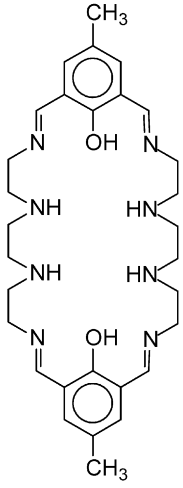

L86

A class of ligands containing phenolic units totally different from the previous one is the family of macrocyclic ligands. Almost all ligands reported contain the phenolic moiety as integral part of the macrocyclic skeleton; **L77** is the only one which shows the phenol as pendant arm of the macrocyclic framework; in particular this ligand can be seen as a molecule formed by two macrocyclic units connected by a phenolic group.

Dinuclear Cu(II) complex of macrocyclic ligand **L71** was obtained using an interesting synthetic procedure which involves a direct single pot template synthesis using the copper(II) nitrate, 1,2-diaminoethane, 4-methyl-2,6-diformylphenol, and sodium azide as reagents [13]. The complex was easily obtained with moderate yields. X-ray structure analysis revealed that the two Cu(II) ions are in a distorted square pyramidal coordination environment with the two phenoxide oxygen atom which adopt a bridge disposition between the two metal centres (see Fig. 27)

The topology of the symmetric ligand **L71** forces the two metal ions to stay close to each other, with a Cu–Cu separation of 2.913 Å. Interestingly, this dinuclear complex exhibits a supramolecular 2D assembly through hydrogen bonding, as shown in packing diagram reported in Fig. 28.

Asymmetrical compartimental ligands are of great interest because they provide discrete heterodinuclear core complexes. These complexes are interesting for their potential use in solvatochromism studies and for their catalytic activities. A very recent example of a asymmetrical macrocyclic ligand involved in the formation of heterodinuclear complexes is **L72**. Ligand **L72** contains two phenolic moieties and it can be considered a dicompartimental ligand which shows hexa- and pentadentate coordination sites that give peculiar characteristics to the whole molecule. In fact, a novel macrobicyclic heterodinuclear Zn(II)–Ni(II) complex, has been recently reported [58]. The structure reveals an asymmetrical nature with the two different binding areas of the ligand involved in the coordination of the two different metal ions. The Ni(II) ion occupies a square planar geometry and it is bound to an iminic and aminic nitrogen atoms of the diethylenetriamine link as well as to two phenolic oxygen atoms. The formation of this asymmetrical structure mainly arises from the chelate ring size. As a consequence, both

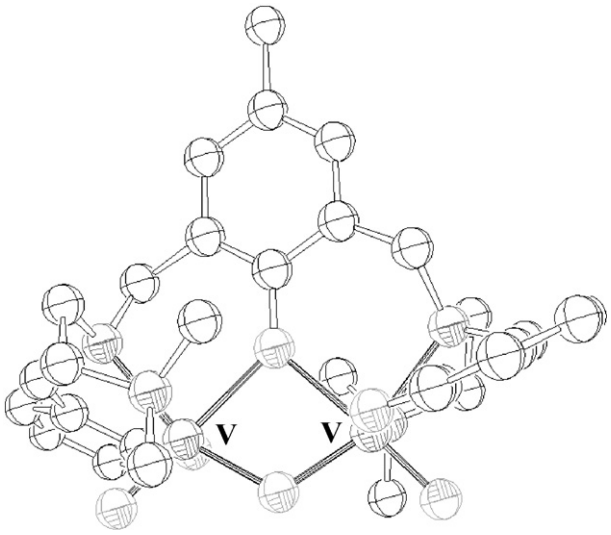

Fig. 26. ORTEP view of the $[V_2(H_{-3}\mathbf{L64})(\mu\text{-}O)(O)_2]$ species.

the pyridyl ligands dispose themselves to the same side of the mean molecular plane towards to that of the phenolic groups. In this complex the Zn–Ni intermetallic separation bridged by both phenolic oxygen atoms is 3.104 Å.

An example of a more complex molecule is the large polyaza-phenolic-macrobicycle **L73**. This ligand can be considered as formed by the large polyazamacrocyclic base [24] $aneN_8$ bridged at two opposite amine functions by the 2,6-dimethyl-phenolic unit. The ligand has been studied in its coordinating properties towards Cu(II) and Zn(II) ions by means

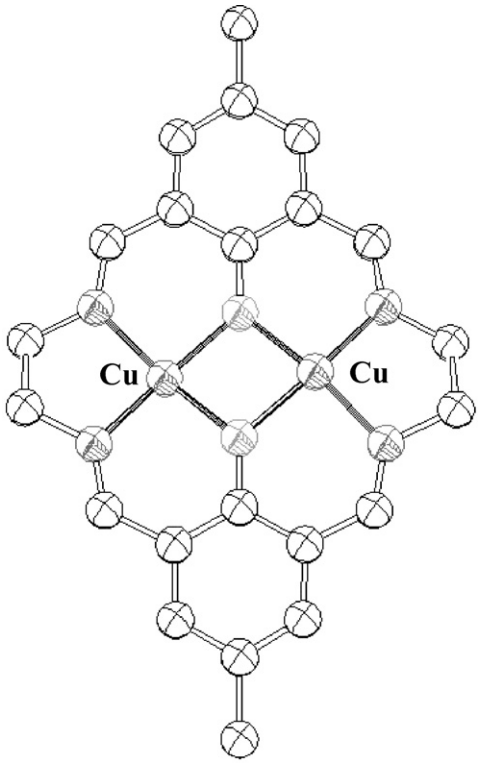

Fig. 27. ORTEP view of $[Cu_2H_{-2}\mathbf{L71}(N_3)_2]\cdot 2H_2O$.

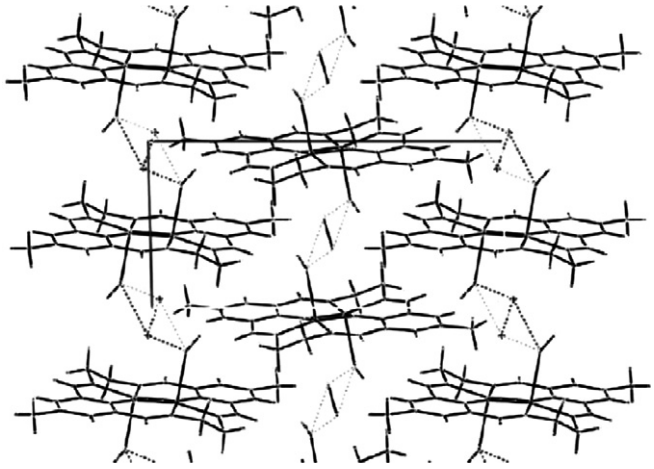

Fig. 28. Supramolecular 2D assembly of complex $[Cu_2\mathbf{L71}(N_3)_2]\cdot 2H_2O$.

of potentiometric measurements in aqueous solution (298.1 K, $I = 0.15$ mol dm^{-3}) [59]. The equilibrium constants determined are reported in Table 12.

The high value of the log K relative to the addition of a second metal ion for both Cu(II) and Zn(II) to the mononuclear $[M(H_{-1}\mathbf{L73})]^+$ species highlight the great tendency of this ligand to coordinate another M(II) ion, forming stable dinuclear species that are the only species existing in solution at pH higher than 6 when the ligand to metal ratio is 1:2. The two metal ions are coordinated by the amine functions and by the phenolate oxygen moiety that bridges the two M(II) ions. This has been confirmed by the crystal structure of the dinuclear $[Zn_2(H_{-1}\mathbf{L73})]^{3+}$ species. The two Zn(II) ions are 3.331 Å apart and each metal ion is pentacoordinated by the four nitrogen atoms provided by the polyaza macrobicycle and the phenolic oxygen atom, as illustrated in Fig. 29.

The crystal structure shows also that the cage topology of ligand **L73** well isolates the metal ions from the medium, with the donor atoms of the ligand fulfilling the coordination requirement of the two Zn(II) ions lodging inside the three-dimensional cavity. This aspect reflects the tendency to add OH^-. In fact, the formation constants of the hydroxylated $[M_2(H_{-1}\mathbf{L73})OH]^{2+}$ species are low (reaction $[M_2(H_{-1}\mathbf{L73})]^{3+} + OH^- = [M_2(H_{-1}\mathbf{L73})OH]^{2+}$; log $K = 2.50$ and 2.83 for Cu(II) and Zn(II), respectively).

Example of asymmetric macrocyclic ligands that has been recently reported by Tamburini et al. are ligands **L74** [60] and

Table 12
Logarithm of the equilibrium constants determined in 0.15 mol dm^{-3} NMe_4NO_3 at 298.1 K for the complexation reactions of **L73** with Cu(II) and Zn(II) ions

Reaction	log K	
	Cu(II)	Zn(II)
$2M^{2+} + \mathbf{L73} = M_2\mathbf{L73}^{4+}$	33.76(2)[a]	21.23(1)
$2M^{2+} + \mathbf{L73} + H_2O = M_2(H_{-1}\mathbf{L73})OH^{2+} + 2H^+$	19.88(4)	5.43(2)
$M^{2+} + M\mathbf{L73}^{2+} = M_2\mathbf{L73}^{4+}$	11.63	5.68
$M^{2+} + M(H_{-1}\mathbf{L73})^+ = M_2(H_{-1}\mathbf{L73})^{3+}$	18.87	11.51
$M_2(H_{-1}\mathbf{L73})^{3+} + OH^- = M_2(H_{-1}\mathbf{L73})OH^{2+}$	2.50(4)	2.83(3)

[a] Values in parentheses are the standard deviations on the last significant figure.

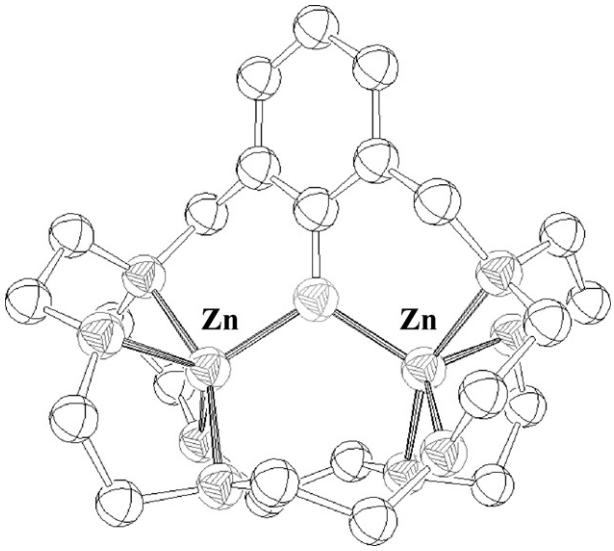

Fig. 29. ORTEP view of the complex cation $[Zn_2(H_{-1}\mathbf{L73})]^{3+}$.

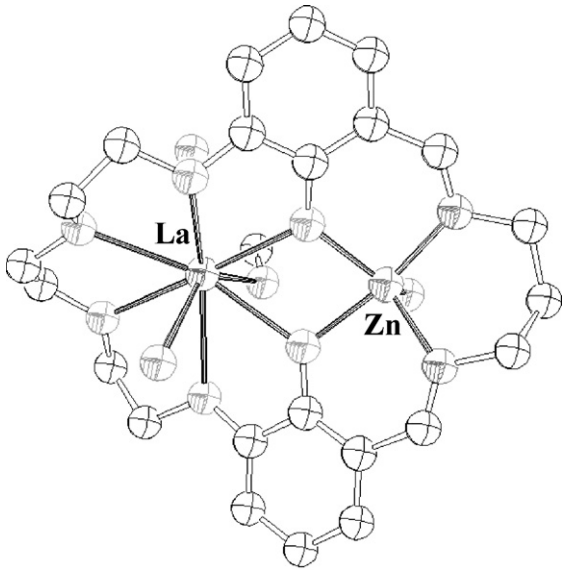

Fig. 30. ORTEP view of the complex cation $[LaZn(H_{-2}\mathbf{L75})]^{3+}$.

L75 [61]. **L74** is a compartmental ligand which is capable to bind two equal or different metal ions in close proximity; in fact, a molecule of this kind offers the possibility to give two different recognition processes in the two adjacent sites. In this way, numerous hetero-dinuclear complexes with similar ligands were prepared. Ligand **L74** was used in the synthesis of $[LnLn'(H_{-2}\mathbf{L74})]Cl_4$ complexes, where LnLn′ = CeEu, EuCe, EuLu, EuYb and YbEu. Generally these hetero-dinuclear complexes have low solubility in methanol, and an increased solubility is generally correlated to demetalation processes, with the consequent formation of the more soluble mononuclear species. Homodinuclear complexes of this ligand were also synthesized. Complex $[Eu_2(H_{-2}\mathbf{L74})Cl_4]\cdot 4H_2O$, obtained by template procedure, was the only homodinuclear complex enough soluble to allow NMR investigations. Ligand **L75** formed heterodinuclear metal complexes which have been also characterized by X-ray crystallography. The ORTEP view of the complex $[LaZn(H_{-2}\mathbf{L75})]Cl_3\cdot CH_3OH$ is reported in Fig. 30.

The Zn(II) ion resides in the N_2O_2 site in a square-pyramidal coordination, the fifth apical position being filled by a chloride ion, while the lanthanum ion is located in the oxygen rich site and is nona-coordinated. Ligand **L75** has an appropriate shape for forming stable heterodinuclear species. Furthermore, the large difference between the two adjacent chambers assures the formation of only one species of heterodinuclear complexes, avoiding transmetallation, scrambling, migration reactions.

A recent work by Okawa et al. reported the template synthesis of a new macrocyclic ligand (**L76**) derived from the cyclic condensation of four molecules of 3-aminomethyl-5-methylsalicylaldehyde in the presence of different metal ions [62]. When Ni(II) was used, two tetranuclear complexes, $[Ni_4(H_{-4}\mathbf{L76})(OH)(H_2O)_4](ClO_4)_3$ and $[Ni_4(H_{-4}\mathbf{L76})(O)(DMF)_4](ClO_4)_2$ have been obtained. Furthermore, the dinuclear $[Mn_2(H_{-2}\mathbf{L76})OH)(AcO)_2(H_2O)]Br$ complex has been produced by a similar condensation in the presence of Mn(II) in open air. X-ray crystallographic studies for $[Ni_4(H_{-4}\mathbf{L76})(OH)H_2O)_8](ClO_4)_3\cdot 7H_2O$ indicate that the macrocyclic ligand accommodates four Ni(II) ions, producing a square Ni_4 core with μ_4-hydroxo group at the center of the core. Each Ni(II) is bound to the exogenous μ_4-hydroxo oxygen and to the ONO donor set of the macrocyclic ligand, with the phenolic oxygen atom that bridges two Ni(II) ions. Water molecules occupy the axial sites of each Ni affording a nearly octahedral geometry about the metal. Magnetic studies for the complexes indicate a ferromagnetic interaction between the adjacent Ni(II) centres and an antiferromagnetic interaction between the diagonal Ni(II) centres. The Mn(III) complex shows a weak antiferromagnetic interaction between the Mn(III) ions, as observed in similar (μ-oxo)bis(μ-carboxylato)-dimanganese(III) complexes.

Recently, the synthesis and the coordination properties of the new macrocyclic ligand **L77** were reported [63]. Equilibrium studies of basicity and coordination properties towards the Cu(II), Zn(II), Cd(II) and Pb(II) ions were performed by potentiometric measurements in aqueous solution (298.1 K, $I = 0.15$ mol dm^{-3}). In Table 13 selected formation constants of different metal ions are reported.

The symmetric molecular topology of ligand **L77**, showing two macrocyclic subunits linked by a phenolic group, is ideal for the formation of dinuclear complexes: **L77** forms stable dinuclear complexes with all of the metal ions investigated, with the phenolate group bridging the two metal ions. This configuration allows the two metal centres to be close to each other in a coordination environment which is still unsaturated. Indeed, the dinuclear species $[M_2(H_{-1}\mathbf{L77})]^{3+}$ (with M = Cu(II), Zn(II) and Pb(II)) shows a great tendency to add the OH^- group and to form dinuclear hydroxo species such as $[M_2(H_{-1}\mathbf{L77})(OH)]^{2+}$. The role of the phenolate oxygen atom in the stabilization *via* a bridging disposition of both metal ions was confirmed by UV/vis studies. Direct evidence of this coordinative behaviour of the ligand **L77** was given from the crystal structures obtained with Ni(II) and Cu(II) ions. In Fig. 31 the ORTEP view of the dinuclear Cu(II) complex with ligand **L77** is reported.

Table 13
Formation constants (log K) of **L77** with Cu(II), Zn(II), Cd(II) and Pb(II) ions in H_2O at 298.1 K, $I = 0.15$ mol dm^{-3} NaCl

Reaction	log K			
	Cu	Zn	Cd	Pb
$MH_{-1}\mathbf{L77}^{+} + M^{2+} = M_2H_{-1}\mathbf{L77}^{3+}$	6.00(1)[a]	8.01(1)	11.91(1)	9.89(1)
$M_2H_{-1}\mathbf{L77}^{3+} + OH^{-} = M_2H_{-1}\mathbf{L77}(OH)^{2+}$	4.77(3)	5.66(3)	2.8(1)	3.18(2)
$M_2H_{-1}\mathbf{L77}(OH)^{2+} + OH^{-} = M_2H_{-1}\mathbf{L77}(OH)_2^{+}$	–	2.72(2)	–	–

[a] Values in parentheses are the standard deviations on the last significant figure.

The way in which the $H_{-1}\mathbf{L77}^{-}$ species is wrapped around the metal ions filling, albeit only partially, their coordination sites is almost identical in both the metal complexes. The phenolic oxygen atom acts as bridging unit between the two metal ions, keeping the Ni(II) and the (Cu(II) ions in close proximity (3.150 and 3.118 Å, respectively). The restricted number of donors (four) supplied by the ligand to each metal ion and the closeness of the two metal cations allow the latter to host external species in order to complete their coordination spheres.

The larger macrocyclic ligand **L78** has been synthesized by Martell et al. by $NaBH_4$ reduction of the Schiff base obtained from [2 + 2] template condensation of 2,6-diformyl-*p*-cresol with diethylenetramine [64]. Complexes formed with this ligand have been extensively studied both in solid state than in solution [65]. **L78** is a very flexible ligand that forms dinuclear complexes with Cu(II) and Ni(II) ions having different characteristics. In the homodinuclear copper complex the two metal ions are located in separate compartments and each of them is coordinated to three amino nitrogen atoms deriving from two diethylenetriamine units and to one phenolic oxygen atom which is not involved in a bridged disposition. As a consequence of this coordinative pattern the Cu–Cu distance is 5.36 Å. On the contrary, when the metal ion is Ni(II) the structure is quite different.

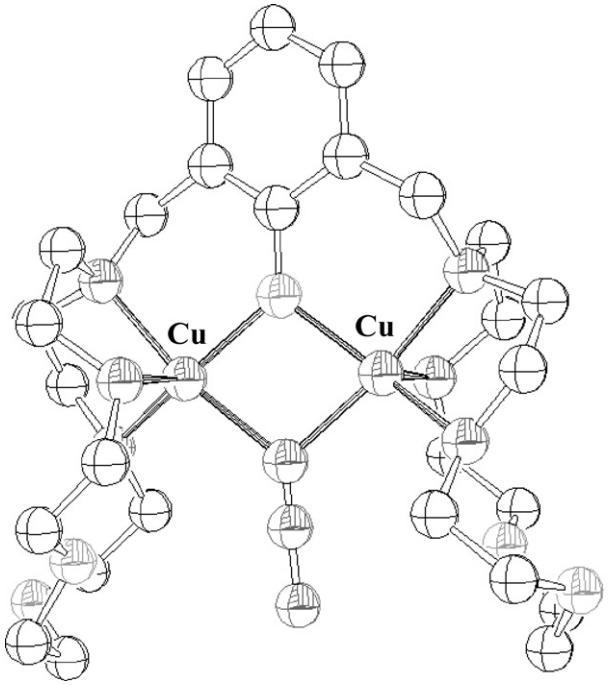

Fig. 31. ORTEP view of the complex cation $[Cu_2(H_{-1}\mathbf{L77})(N_3)]^{2+}$.

In fact, each Ni(II) ion is coordinated by three amino nitrogen atoms, two bridged phenolic oxygen atoms and an oxygen deriving from a water molecule. The Ni(II)–Ni(II) separation for this complex is 3.14 Å.

The potentiometric equilibrium studies, performed in aqueous solution (298.1 K, $I = 0.10$ mol dm^{-3}), indicate that the homodinuclear nickel complexes with the two phenolic oxygen atoms combined with the central nickel atoms via oxo-bridges predominate from pH 10.0 to 12.0. The stability constant of the dinuclear complex with fully deprotonated ligand is $\log K_{[Ni2H-2\mathbf{L78}]/[NiH-2\mathbf{L78}][Ni]} = 10.85$. When the metal ion is copper the system is much simpler than the corresponding Ni(II) system. Above pH 4.3 the fully deprotonated dinuclear complex $[Cu_2(H_{-2}\mathbf{L78})]^{2+}$ becomes the major species; no hydroxo copper complexes have been found in the whole pH range on account of its high stability constant: $[Cu]^{2+} + [Cu(H_{-2}\mathbf{L78})] = [Cu_2(H_{-2}\mathbf{L78})]$ $\log K = 21.75$. Ligand **L78** forms also dinuclear complexes with Fe(II,II) and Fe(III,III) metal ions. Potentiometric data indicate that the formation of a μ-oxo bridge between two ferric ions in the dinuclear species occurs even under fairly acidic conditions: between pH 4 and 7, the stable μ-hydroxo-bridged diferric complex $[Fe(III)_2(\mu\text{-}OH)(H_{-2}\mathbf{L77})]^{3+}$ predominates, and the μ-oxo-bridged diferric complexes become the main component in an aqueous solution at high pH values. Mixed-valence dinuclear Fe(II,III) complexes have also been studied. These dinuclear ferrous complexes have been tested in the catalytic hydroxylation of adamantane in the presence of a two-electron reductant (H_2S). The overall oxidation reactions are shown in Scheme 5.

This macrocyclic iron complex was less active with respect other iron complexes formed with more rigid ligands; moreover, the oxidation of adamantane produced not only hydroxylation but also ketonization products when the reaction was performed in CH_3CN. When the solvent was changed to acetone, in the same experimental conditions, no ketonization products were detected.

Yan et al. also studied the macrocyclic ligand **L78** obtaining the complex $[Ni_2(H_{-2}\mathbf{L78})](ClO_4)_2$ by the reaction of $Ni(ClO_4)_2$ and **L78** [66]. Differently from the structure obtained by Martell et al., this complex revealed to be formed by two Ni(II) centres bridged by two phenoxide oxygen atoms completing the Ni_2O_2 plane. Each of the metal centres obtains a five coordinated environment by interacting with three secondary amine nitrogen donors. The two nickel atoms are separated by 3.092 Å. The thermal decomposition processes of this complex were studied using TG–DTG and the kinetic parameters were

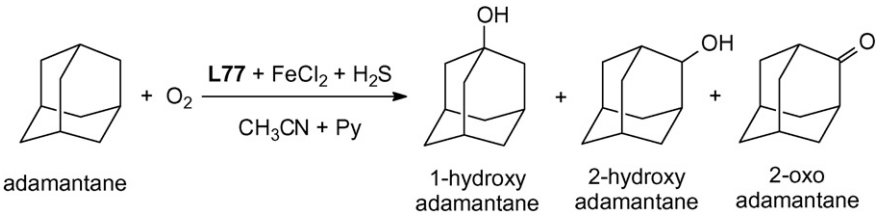

Scheme 5. Oxidation of adamantane by molecular dioxygen with dinuclear iron(II) complexes as catalysts.

obtained from analysis of the curves with integral and differential methods [67].

The macrocyclic ligands **L79** and **L80** have been synthesized through the 2 + 2 condensation of 2,6-diformyl-*p*-cresol with appropriate diamines; the following reduction of the tetra Schiff base afforded the saturated macrocycles **L79** and **L80** [68]. These ligands form dinuclear Fe(II) and Fe(III) complexes in which the Fe(II) and Fe(III) centres are coordinated and bridged by the phenolate groups. Potentiometric equilibrium studies, performed in KCl supporting electrolyte (0.1 mol dm^{-3}) at 298.1 K, indicate for the ligand **L79** that a variety of mononuclear and dinuclear Fe(II) and Fe(III) complexes form through pH 2 to 11 in aqueous solution are forming. Three different dinuclear complexes were identified with fairly high stability constants for the ferrous ion-ligand system. At pH > 7 only dinuclear species exist in solution, whereas the hydroxo-bridged species $[Fe(II)_2(\mu\text{-OH})(H_{-2}\mathbf{L79})]^{+}$ predominates over pH 10. In the case of ferric ion, stable μ-hydroxo bridged are observable even under fairly acidic conditions: the $[Fe(III)_2(\mu\text{-OH})(H_{-2}\mathbf{L79})]^{3+}$ species is prevalent between pH 3.5 and 7. Above pH 7, the μ-oxo bridged diferric complex $[Fe(III)_2(\mu\text{–O})(H_{-2}\mathbf{L79})]^{2+}$ and its further hydrolytic species become the main components in aqueous solution. The dinuclear Fe(II) complexes of the ligands **L79** and **L80** catalyze the hydroxylation of hydrocarbons (cyclohexane and adamantane) by molecular oxygen, in the presence of H_2S as a two-electron reductant [69]. The hydrocarbons are mainly hydroxylated, also if some ketonization products are observable in the case of cyclohexane. It is interesting that the oxidation of adamantane produces only hydroxylation product; no ketonization product is observed. The turnover numbers are really high and thus these dinuclear macrocyclic iron(II) complexes are among the most effective functional models of methane monooxygenase reported thus far.

One of the few examples of macrocyclic ligand able to form polynuclear metal complexes and containing only one phenolic unit is **L81** [70]. The ligational properties of **L81** towards Ni(II), Zn(II) and Cu(II) ions were determined by means of potentiometric measurements in aqueous solution (298.1, $I = 0.15$ mol dm^{-3}). The ligand form dinuclear species with all the metal ions studied. The addition of the second metal ions to the mononuclear species gave lesser stability constants than the first one, due to the low number of donor atoms present in the ligand. In the case of copper(II) complexes the dinuclear species are largely prevalent in solution at pH values higher than 6. For the Ni(II) and Cu(II) complexes, hydroxylated species were detected and were the prevalent species in solution at alkaline pH. UV spectra recorded in aqueous solution containing **L81** and M(II) in various molar ratios and different pH values supported the hypothesis that the phenol played an important role in the formation of the dinuclear species, due to the capacity of the phenolic oxygen atom to bridge two metal ions, forcing them to stay very close. These results were confirmed by the crystal structure of $[Ni_2(H_{-1}\mathbf{L81})(H_2O)_2Cl_2]^{+}$ cation reported in Fig. 32.

As can be seen in the Fig. 32, the macrocyclic ligand act as a hexadentate, and each Ni atom has an octahedral geometry. The phenolic oxygen atom, together a Cl atom, disposes itself in a bridge disposition between the two metal centres. The distance from the two-nickel atoms is 3.209 Å.

Ligand **L82** is an example of an ncapsulating ligand containing three phenolic groups. This ligand has been synthesized by a metal-templated reaction between triethylammonium 2,6-diformyl-4-methylphenolate and tris(2-aminoethyl)amine in the presence of hydrated lanthanide nitrates (Ln = Gd–Lu) [71]. X-ray crystallographic data were collected in the case of complex $[Lu_2(H_{-3}\mathbf{L82})(NO_3)_2]^{+}$. In the complex the two lutetium(III) ions have the same coordination environment and are at a distance of 3.447 Å. All the three phenolic oxygen atoms bridge the two metals. These constitutes the first examples of dinuclear lanthanide complexes of an iminophenolate cryptand together with the crystal structure of a dilutetium(III) complex.

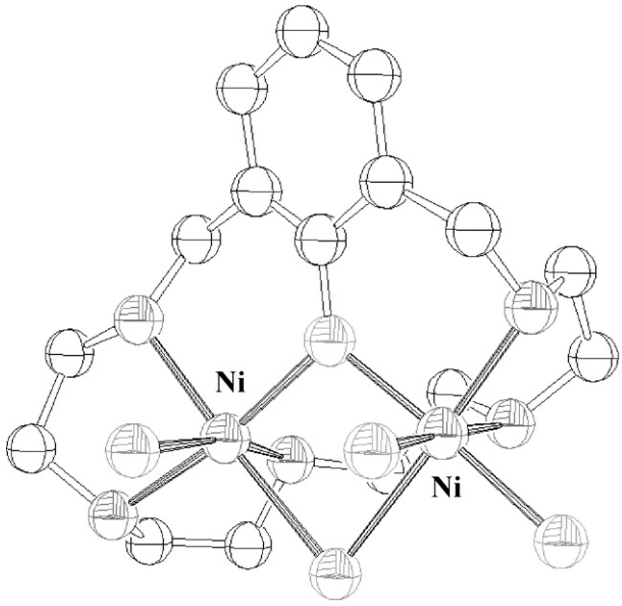

Fig. 32. ORTEP view of the complex cation $[Ni_2(H_{-1}\mathbf{L81})]^{+}$.

Nag et al. reported the synthesis and characterization, together with the coordinative properties, of the homo- and heterodinuclear complexes formed by the ligand **L83** [72]. This ligand easily formed dinuclear metal complexes with Ni(II) ion that have been characterized by X-ray crystallography. Crystal data reveal, in the case of the $[Ni_2(H_{-2}\mathbf{L83})(CH_3OH)_2](ClO_4)_2$ species, that the two Ni(II) centres are bridged by two phenoxide oxygen atoms with two secondary amine nitrogen donors completing the NiN_2O_2 plane [73]. The octahedral environment of the metal centres is completed by the trans axially disposed methanol molecules and perchlorate ions. The two metal centres are separated by 3.135 Å. The high coordination numbers of Ni(II) ion, together with the low number of donor atoms of the ligand **L83**, prompted the authors to study the interaction of this complex with amino acids. The result was the synthesis and characterization of the carboxylate-bridged complex $[Ni_2(H_{-2}\mathbf{L83})(\mu\text{-}^{-}O_2C\text{-}NH_3^{+})(H_2O)_2](ClO_4)_2$, that was the first example of μ-carboxylate binding of amino acids in zwitterionic form in Ni(II) chemistry [74]. The authors studied also the magneto-structural relationship in a series of dinuclear Ni(II) complexes with ligand **L83** [75]. A linear dependence of antiferromagnetic exchange coupling constant ($-J$) on Ni–O–Ni bridge angle as well as the intramolecular Ni···Ni distance has been obtained for the dinickel(II) complexes with centrosymmetric structures. As mentioned before, ligand **L83** was able to form heterodinuclear complexes with transition metal ions. In fact, a series of bimetallic complexes of the type $[Fe(III)M(II)(H_{-2}\mathbf{L83})(\mu\text{-}OAc)(OAc)(H_2O)](ClO_4)\cdot nH_2O$ (where M(II) = Zn, Ni, Co and Mn) and $[\{Fe(III)Co(III)(H_{-2}\mathbf{L83})(\mu\text{-}OAc)(OAc)\}_2(\mu\text{-}O)]ClO_4)_2\cdot 3H_2O$ have been synthesized and characterized. Spectral data indicate that in all the cases the metal ions have similar environments. An in-depth study of the magnetic, spectroscopic and redox properties of these complexes has been performed, and two crystal structures, for complexes $[Fe(III)Ni(II)(H_{-2}\mathbf{L83})(\mu\text{-}OAc)(OAc)(H_2O)](ClO_4)\cdot 2H_2O$ and $[\{Fe(III)Co(III)(H_{-2}\mathbf{L83})(\mu\text{-}OAc)(OAc)\}_2(\mu\text{-}O)]ClO_4)_2\cdot 3H_2O$, allowed to confirm the bridge disposition of the phenoxide oxygen atom between the two metal centres, with a distance of 3.03 and 3.085 Å, respectively.

The macrocyclic ligands **L84** and **L85** have been synthesized by a 2:2 template condensation of 2,6-diformyl-4-(*R*)-phenol (R = Me, *t*Bu) with 3,6-bis(aminoethyl)thio)-pyridazina in the presence of copper(II) salts [76]. Dinuclear Cu(II) complexes of the 34-membered macrocyclic ligands **L84** and **L85** were obtained. These two ligands are potentially decadentate, capable of forming endogenous phenolate and pyridazino bridges and possibly binding four metal centres. The involvement of the sulphur atoms as donors could increase the coordination capacity beyond four. However, in these complexes, the macrocycles coordinate with the familiar N_4O_2, equatorial donor set, to two phenoxide bridged copper(II) centres. The Cu···Cu distance in the complexes formed by **L84** and **L85** were 3.017 and 3.066 Å, respectively. All the complexes were studied in their magnetic and redox properties; in particular, EPR spectra were recorded for all the mixed valence Cu(II)–Cu(I) complexes.

Ligand **L86** is another ligand that has been obtained by a 2:2 template condensation of 2,6-diformyl-*p*-cresol and triethylenetetramine in the presence of lanthanide salts [77]. The magnetic and luminescence properties of the complexes have been studied but all the efforts to obtain crystalline states suitable for X-ray analysis were not successful. The magnetic susceptibility measurements suggested that coupling between lanthanide ions was significant, at least in the case of the praesodymium complexes. The luminescence properties provided considerably more detailed insight into the nature of the complexes. The luminescence from the La^{3+}, Y^{3+} and Gd^{3+} complexes are clearly attributable to emissions from the chromophoric (Schiff base) portion of the macrocyclic ligand; the energy of the emissive excited state was significantly affected by coordination at the phenolate ion and by intermolecular aggregation. Finally, the different coloured forms which the lanthanide complexes showed were attributable to different environments for the chromophoric group.

4. Conclusions

The foregoing pages have illustrated how chemists from different backgrounds have synthesized new molecules with different molecular topology but all having the phenolic group and amines as fragment in their framework.

We hope that this short review will be a handy reference for those already in the field and a stimulating entry point for new researchers.

Acknowledgement

Technical support from Dr. R. Pontellini is gratefully acknowledged.

References

[1] N.H. Pilkington, R. Robson, Aust. J. Chem. 23 (1970) 2225.
[2] N. Ceccanti, M. Formica, V. Fusi, L. Giorgi, M. Micheloni, R. Pardini, R. Pontellini, M.R. Tinè, Inorg. Chim. Acta 321 (2001) 153.
[3] P. Dapporto, M. Formica, V. Fusi, L. Giorgi, M. Micheloni, P. Paoli, R. Pontellini, P. Rossi, Inorg. Chem. 40 (2001) 6186.
[4] G. Ambrosi, M. Formica, V. Fusi, L. Giorgi, A. Guerri, M. Micheloni, R. Pontellini, P. Rossi, Polyhedron 22 (2003) 1135.
[5] P. Dapporto, M. Formica, V. Fusi, M. Micheloni, P. Paoli, R. Pontellini, P. Rossi, Inorg. Chem. 39 (2000) 4663.
[6] L. Chiarantini, A. Cerasi, L. Giorgi, M. Formica, M.F. Ottavini, M. Cangiotti, V. Fusi, Bioconj. Chem. 14 (2003) 1165.
[7] M. Cangiotti, M. Formica, V. Fusi, L. Giorgi, M. Micheloni, M.F. Ottavini, S. Sampaolesi, Eur. J. Inorg. Chem. (2004) 2853.
[8] E. Berti, A. Caneschi, C. Daiguebonne, P. Dapporto, M. Formica, V. Fusi, L. Giorgi, A. Guerri, M. Micheloni, P. Paoli, R. Pontellini, P. Rossi, Inorg. Chem. 42 (2003) 348.
[9] G. Ambrosi, M. Formica, V. Fusi, L. Giorgi, A. Guerri, M. Micheloni, P. Paoli, R. Pontellini, P. Rossi, Inorg. Chim. Acta 356 (2003) 203.
[10] G. Ambrosi, P. Dapporto, M. Formica, V. Fusi, L. Giorgi, A. Guerri, M. Micheloni, P. Paoli, P. Rossi, J. Supramol. Chem. 2 (2002) 301.
[11] M. Du, D.L. An, Y.M. Guo, X.H. Bu, J. Mol. Struct. 641 (2002) 193.
[12] S. Banerjee, M.G.B. Drew, C.Z. Lu, J. Tercero, C. Diaz, A. Ghosh, Eur. J. Inorg. Chem. (2005) 2376.
[13] T. Chattopadhyay, K.S. Banu, A. Banerjee, J. Ribas, A. Majee, M. Nethaji, D. Das, J. Mol. Struct. 833 (2007) 13.

[14] C. Higuchi, H. Sakiyama, H. Okawa, R. Isobe, D.E. Fenton, J. Chem. Soc., Dalton Trans. (1994) 1097.
[15] C. Higuchi, H. Sakiyama, H. Okawa, D.E. Fenton, J. Chem. Soc., Dalton Trans. (1995) 4015.
[16] T. Koga, H. Furutachi, T. Nakamura, N. Fukita, M. Ohba, K. Takahashi, H. Okawa, Inorg. Chem. 37 (1998) 989.
[17] R. Amase, H. Shiraishi, Y. Miyasato, M. Ohba, H. Okawa, Bull. Chem. Soc. Jpn. 78 (2005) 1814.
[18] K. Matsufuji, H. Shiraishi, Y. Miyasato, T. Shiga, M. Ohba, T. Yokoyama, H. Okawa, Bull. Chem. Soc. Jpn. 78 (2005) 851.
[19] K. Abe, J. Izumi, M. Ohba, T. Yokoyama, H. Okawa, Bull. Chem. Soc. Jpn. 74 (2001) 85.
[20] Y. Gultneh, Y.T. Tesema, T.B. Yisgedu, R.J. Butcher, G. Wang, G.T. Yee, Inorg. Chem. 45 (2006) 3023.
[21] M. Lubben, R. Hage, A. Meetsma, B.L. Feringa, Inorg. Chem. 34 (1995) 2217.
[22] M. Ghiladi, C.J. McKenzie, A. Meier, A.K. Powell, J. Ulstrup, S. Wocadlo, J. Chem. Soc., Dalton Trans. (1997) 4011.
[23] I.A. Koval, M. Huisman, A.F. Stassen, P. Gamez, M. Lutz, A.L. Spek, D. Pursche, B. Krebs, J. Reedijk, Inorg. Chim. Acta 357 (2004) 294.
[24] C. Hureau, L. Sabater, E. Anxolabehere-Mallart, M. Nierlich, M. Charlot, F. Gonnet, E. Riviere, G. Blondin, Chem.-Eur. J. 10 (2004) 1998.
[25] A. Greatti, M. Aires de Brito, A.J. Bortoluzzi, A. Ceccato, Augusto J. Mol. Struct. 688 (2004) 185.
[26] S. Chardon-Noblat, O. Horner, B. Chabut, F. Avenier, N. Debaecker, P. Jones, J. Pecaut, L. Dubois, C. Jeandey, J. Oddou, A. Deronzier, J. Latour, Inorg. Chem. 43 (2004) 1638.
[27] H. Adams, D.E. Fenton, P.E. McHugh, T.J. Potter, Inorg. Chim. Acta 331 (2002) 117.
[28] Z. Tyeklar, P.P. Paul, R.R. Jacobson, A. Farooq, K.D. Karlin, J. Zubieta, J. Am. Chem. Soc. 111 (1989) 388.
[29] J. Costes, F. Dahan, A. Dupuis, J. Laurent, Inorg. Chem. 39 (2000) 169.
[30] S.M. Couchman, J.C. Jeffery, P. Thornton, M.D. Ward, J. Chem. Soc., Dalton Trans. (1998) 1163.
[31] C.A. Otter, D.A. Bardwell, S.M. Couchman, J.C. Jeffery, J.P. Maher, M.D. Ward, Polyhedron 17 (1998) 211.
[32] Y. Maeda, K. Kawano, T. Oniki, J. Chem. Soc., Dalton Trans. (1995) 3533.
[33] M.R. Maurya, A. Kumar, M. Ebel, D. Rehder, Inorg. Chem. 45 (2006) 5924.
[34] P. Amudha, P. Akilan, M. Kandaswamy, Polyhedron 18 (1999) 1355.
[35] F.M. Nie, R.J. Wang, Y.M. Li, Y.F. Zhao, M. Nethaji, A.R. Chakravarty, Chin. Chem. Lett. 9 (1998) 881.
[36] M. Rapta, P. Kamaras, G.A. Brewer, G.B. Jameson, J. Am. Chem. Soc. 117 (1995) 12865.
[37] S.K. Dutta, K.K. Nanda, U. Floerke, M. Bhadbhade, K. Nag, J. Chem. Soc., Dalton Trans. (1996) 2371.
[38] N. Koprivanac, A. Metes, S. Papic, B. Kralj, Spectrosc. Lett. 29 (1996) 27.
[39] I.A. Koval, M. Huisman, A.F. Stassen, P. Gamez, P.O. Roubeau, C. Belle, J. Pierre, E. Saint-Aman, M. Lueken, B. Krebs, M. Lutz, A.L. Spek, J. Reedijk, Eur. J. Inorg. Chem. (2004) 4036.
[40] H. Sakiyama, T. Suzuki, K. Ono, R. Ito, Y. Watanabe, M. Yamasaki, M. Mikuriya, Inorg. Chim. Acta 358 (2005) 1897;
H. Sakiyama, Y. Watanabe, R. Ito, Y. Nishida, Inorg. Chim. Acta 357 (2004) 4309;
H. Sakiyama, Y. Igarashi, Y. Nakayama, J. Hossain, K. Unoura, Y. Nishida, Inorg. Chim. Acta 351 (2003) 256;
J. Hossain, M. Yamasaki, M. Mikuriya, A. Kuribayashi, H. Sakiyama, Inorg. Chem. 41 (2002) 4058;
H. Sakiyama, R. Ito, H. Kumagai, K. Inoue, M. Sakamoto, Y. Nishida, M. Yamasaki, Eur. J. Inorg. Chem. (2001) 2027;
H. Sakiyama, R. Mochizuki, A. Sugawara, M. Sakamoto, Y. Nishida, M. Yamasaki, J. Chem. Soc., Dalton Trans. (1999) 997.
[41] P.M. Bruce, D.B. Pauil, Q. Lawrenc, J. Am. Chem. Soc. 107 (1985) 6728.
[42] O. Horner, E. Anxolabehere-Mallart, M. Charlot, L. Tchertanov, J. Guilhem, T.A. Mattioli, A. Boussac, J. Girerd, Inorg. Chem. 38 (1999) 1222;
L. Sabater, C. Hureau, G. Blain, R. Guillot, P. Thuery, E. Riviere, A. Aukauloo, Eur. J. Inorg. Chem. (2006) 4324.
[43] I.A. Koval, M. Sgobba, M. Huisman, M. Lueken, E. Saint-Aman, P. Gamez, B. Krebs, J. Reedijk, Inorg. Chim. Acta 359 (2006) 4071.
[44] S. Ma, X. Sun, S. Gao, C. Qi, H. Huang, W. Zhu, Eur. J. Inorg. Chem. (2007) 846.
[45] G. Aromi, H. Stoeckli-Evans, S.J. Teat, J. Cano, J. Ribas, J. Mater. Chem. 16 (2006) 2635.
[46] M.F. Anderlund, J. Hoegblom, W. Shi, P. Huang, L. Eriksson, H. Weihe, S. Styring, B. Aakermark, R. Lomoth, A. Magnuson, Eur. J. Inorg. Chem. (2006) 5033.
[47] H. Zhang, K. Ye, J. Zhang, Y. Liu, Y. Wang, Inorg, Chem. 45 (2006) 1745.
[48] K. Manseki, H. Sakiyama, M. Sakamoto, Y. Nishida, H. Aono, Y. Sadaoka, M. Ohba, H. Okawa, Synth. React. Inorg. Met.-Org. Chem. 31 (2001) 1443.
[49] G. Ambrosi, M. Formica, V. Fusi, L. Giorgi, A. Guerri, M. Micheloni, P. Paoli, R. Pontellini, P. Rossi, Inorg. Chem. 46 (2007) 309.
[50] I. Brady, D. Leane, H.P. Hughes, R.J. Forster, T.E. Keyes, Dalton Trans. (2004) 334.
[51] H. Sopo, J. Sviili, A. Valkonen, R. Sillanpaeae, Polyhedron 25 (2006) 1223.
[52] G.M. Meppelder, T.P. Spaniol, J. Okuda, J. Organomet. Chem. 691 (2006) 3206.
[53] M.R.A. Pillai, C.L. Barnes, E.O. Schlemper, Polyhedron 13 (1994) 701;
M.R.A. Pillai, C.S. John, J.M. Lo, E.O. Schlemper, D.E. Troutner, Inorg. Chem. 29 (1990) 1850.
[54] H. Adams, D. Bradshaw, D.E. Fenton, J. Chem. Soc., Dalton Trans. (2002) 925.
[55] C. Zhanfen, W. Xiayong, C. Jingwen, Y. Xiaoliang, L. Yizhi, G. Zijian, New J. Chem. 31 (2007) 357.
[56] A. Mondal, S. Sarkar, D. Chopra, T.N.G. Row, K. Pramanik, K.K. Rajak, Inorg. Chem. 44 (2005) 703.
[57] H. Li, F. Shi, X. Peng, R. Zhang, X. Chen, L. Zhang, L. Sun, Huaxue Xuebao 62 (2004) 916.
[58] H. Golchoubian, E. Baktash, R. Welter, Inorg. Chem. Commun. 10 (2007) 120.
[59] G. Ambrosi, P. Dapporto, M. Formica, V. Fusi, L. Giorgi, A. Guerri, M. Micheloni, P. Paoli, R. Pontellini, P. Rossi, Inorg. Chem. 45 (2006) 304.
[60] S. Tamburini, P.A. Vigato, M. Gatos, L. Bertolo, U. Casellato, Inorg. Chim. Acta 359 (2006) 183.
[61] A. Caneschi, L. Sorace, U. Cesellato, P. Tomasin, P.A. Vigato, Eur. J. Inorg. Chem. (2004) 3887.
[62] K. Ikeda, K. Matsufuji, M. Ohba, M. Kodera, H. Okawa, Bull. Chem. Soc. Jpn. 77 (2004) 733.
[63] G. Ambrosi, P. Dapporto, M. Formica, V. Fusi, L. Giorgi, A. Guerri, M. Micheloni, P. Paoli, R. Pontellini, P. Rossi, Dalton Trans. (2004) 3468.
[64] D. Kong, A.E. Martell, R.J. Motekaitis, Ind. Eng. Chem. Res. 39 (2000) 3429.
[65] D. Kong, A.E. Martell, R.J. Motekaitis, J.H. Reibenspies, Inorg. Chim. Acta 317 (2001) 243.
[66] W. Yan, C. Ma, J. Wu, W. Zhang, D. Jiang, Inorg. Chim. Acta 287 (1999) 212.
[67] W. Yan, C. Ma, J. Wu, W. Zhang, D. Jiang, J. Therm. Anal. Calorim. 58 (1999) 393.
[68] Z. Wang, A.E. Martell, R.J. Motekaitis, J.H. Reibenspies, J. Chem. Soc., Dalton Trans. (1999) 2441.
[69] Z. Wang, A.E. Martell, R.J. Motekaitis, J.H. Reibenspies, Inorg. Chim. Acta 300–302 (2000) 378.
[70] P. Dapporto, M. Formica, V. Fusi, M. Micheloni, P. Paoli, R. Pontellini, P. Romani, P. Rossi, Inorg. Chem. 39 (2000) 2156.
[71] F. Avecilla, A. de Blas, R. Bastida, D.E. Fenton, J. Mahia, A. Macias, C. Platas, A. Rodriguez-Blas, Chem. Commun. (1999) 125.
[72] S.K. Dutta, R. Werner, U. Florke, S. Mohanta, K.K. Nanda, W. Haase, K. Nag, Inorg. Chem. 35 (1996) 2292.
[73] R. Das, K. Nag, Inorg. Chem. 30 (1991) 2831.
[74] R. Das, K.K. Nanda, K. Venkatsubramanian, P. Paul, K. Nag, J. Chem. Soc., Dalton Trans. (1992) 1253.
[75] K.K. Nanda, L.K. Thompson, J.N. Bridson, K. Nag, J. Chem. Soc., Chem. Commun. (1994) 1337.
[76] S.S. Tandon, L.K. Thompson, J.N. Bridson, Inorg. Chem. 32 (1993) 32.
[77] I.A. Kahwa, J. Selbin, C.J. O'Connor, J.W. Foise, G.L. McPherson, Inorg. Chim. Acta 148 (1988) 265.